Geochemical evidence for a subducted infant arc in Franciscan high-grade-metamorphic tectonic blocks

Aniki Saha[†]
Asish R. Basu[‡]
Department of Earth and Environmental Sciences, University of Rochester, Rochester, New York 14627, USA

John Wakabayashi[§]
1329 Sheridan Lane, Hayward, California 94544, USA

Gregory L. Wortman[#]
Department of Earth and Environmental Sciences, California State University, Fresno, California 93740, USA

ABSTRACT

Some of the evidence of tectonic and chemical processes that occur in subduction zones is preserved in blueschists and eclogites, as validated by the geochemical data presented from high-grade-metamorphic tectonic blocks from the Franciscan Complex in central California. Combining major elements, compatible and incompatible trace element concentrations and ratios, and Sr-Nd-Pb isotopic data, we conclude that the protoliths of these high-grade Franciscan blocks were arc lavas with no continental crust–derived components. Although the protoliths underwent high-grade metamorphism at the inception of subduction, the tectonic affinity of the protoliths can be distinguished by our geochemical study. Our geochemical data are significant in that (1) the protoliths of these high-grade blocks have a different mode of origin than the protoliths of the lower-grade Franciscan basalts that were incorporated later in the subduction complex, as the latter generally are considered to be oceanic-island basalts (OIB) and derived from mid-oceanic-ridge basalt (MORB); and (2) the protoliths of the high-grade blocks were formed over a pre-Franciscan subduction zone.

Based on the geochemical evidence for an arc origin and the available geochronological data, we suggest that protoliths of the high-grade tectonic blocks of the Franciscan Complex and the Coast Range Ophiolite formed in the same infant-arc setting. Initiation of Franciscan subduction in this arc crust led to the formation of the high-grade blocks beneath the young Coast Range Ophiolite. Continued subduction resulted in subduction of older oceanic crust of MORB and OIB origin, some of which was scraped off to form lower-grade metabasites within the Franciscan Complex.

Keywords: Franciscan, arc, subduction, geochemistry, high-grade metamorphism.

INTRODUCTION

Physical and chemical processes that occur during subduction contribute significantly to continental growth and geochemical and thermal evolution of Earth's mantle. Subduction is one of the principal mechanisms for the chemical differentiation and evolution of the crust-mantle system and delivers oceanic basaltic crust produced at mid-ocean ridges and sediments deposited on the oceanic crust to the upper mantle. The sequence of metamorphic reactions within the subducting crust is well understood in terms of petrologic-thermal modeling, including the trace element geochemistry of some fluid-mobile elements (Peacock, 1990; Tatsumi and Eggins, 1995). Acting as a flux, fluids released from dehydration of subducted crust assist in the partial melting of mantle peridotites and in the generation of arc magmas. A major source of geochemical information for these processes is from the isotopic and chemical composition of lavas and related magmatic rocks from within convergent margin settings. However, the most direct evidence for the subducted rocks, their compositions, and fluid activity in subduction zones is preserved in the metamorphic rocks from paleosubduction zones.

Blueschists and eclogites, derived from depths of 20 to >100 km, possibly best characterize paleosubduction zones, and they are thought to directly indicate the composition of the subducting oceanic lithosphere and its various lithic components, including subducted sediments as well as fluid-rock interaction. With this perspective, we have conducted an Nd, Sr, and Pb isotopic and major element and multiple trace element study involving the rare earth elements (REE), some large ion lithophile elements (LILE), and high-field-strength elements (HFSE) of the coarse-grained blueschists, amphibolites, and eclogites (so-called high-grade blocks) of the Franciscan Complex in central California.

This study attempts to identify the protoliths of Franciscan blueschists and eclogites and whether there were any oceanic, arc-derived, or old continental crust–derived sediments in their protoliths. Answers to these questions would also help in evaluating the tectono-metamorphic history of the high-grade blocks and how it relates to general processes of subduction initiation and ophiolite emplacement. Our approaches in answering these questions employ measurements of major elements, multiple trace elements, and Nd, Sr, and Pb isotopic ratios. It is well known that multiple elements of different compatibility-incompatibility can be used to distinguish normal mid-oceanic-ridge basalt (N-MORB) and oceanic-island basalt (OIB), as well as arc basalts and sediments. Similarly, the radiogenic isotopes of Sr, Nd, and Pb are sensitive tracers of source rocks, including sedimentary protoliths. Following this approach, we show here that for the high-grade tectonic blocks of the Franciscan, primitive arc basalts were their precursor.

[†]E-mail: aniki@earth.rochester.edu.
[‡]Corresponding author e-mail: abasu@earth.rochester.edu.
[§]Email: wako@tdl.com.
[#]Present address: PANalytical Inc., 12 Michigan Drive, Natick, Massachusetts 01760, USA; e-mail: Gregory.Wortman@panalytical.com.

GSA Bulletin; September/October 2005; v. 117; no. 9/10; p. 1318–1335; doi: 10.1130/B25593.1; 10 figures; 2 tables.

GEOLOGIC SETTING OF HIGH-GRADE BLOCKS IN THE FRANCISCAN COMPLEX

The Franciscan Complex is perhaps the world's best-known subduction complex (Fig. 1A). It formed during a period of >140 m.y. of east-dipping subduction in coastal California from 160 Ma to <20 Ma (Ernst, 1984; Wakabayashi, 1992). The Franciscan Complex is also well known for its high-pressure–low-temperature (HP-LT) metamorphism (Ernst, 1970, 1971b); at least 25% of the exposed rocks have undergone HP-LT blueschist or higher-grade metamorphism (Wakabayashi, 1999). The highest grade metamorphic rocks of the complex are coarse-grained blueschists, eclogites, and amphibolites that occur almost entirely as tectonic blocks in shale or serpentinite-matrix mélanges. Although these high-grade blocks make up <1% of Franciscan metamorphic rocks, they are widely distributed, occurring at hundreds of localities along the length of the exhumed subduction complex (Coleman and Lanphere, 1971).

The Coast Range Ophiolite structurally overlies the Franciscan and is depositionally overlain by well-bedded sandstones and shales of the Great Valley Group that are coeval with the Franciscan (Dickinson, 1970). The Coast Range Ophiolite and Great Valley Group lack HP-LT metamorphism. From west to east, the three subparallel geologic provinces of the Franciscan, the Great Valley Group, and the Sierra Nevada batholith (see Fig. 1A) represent, respectively, the subduction complex, forearc basin deposits, and the magmatic arc of an ancient arc-trench system (Dickinson, 1970). Franciscan lithologies are predominantly detrital sedimentary rocks with subordinate basaltic volcanic rocks and chert, and minor limestone. The detrital rocks are offscraped and underplated trench-fill sediments (Dickinson, 1970). The pelagic and volcanic rocks apparently represent fragments of seamounts, other oceanic rises, and the pelagic cover and upper part of the subducted oceanic crust (Hamilton, 1969; MacPherson, 1983; Shervais, 1990), probably with a component of olistostrome blocks from the upper plate (MacPherson et al., 1990; Erickson et al., 2004).

Franciscan rocks have been traditionally classified as coherent mappable bodies or mélange units that consist of a sheared matrix with included blocks (Blake et al., 1988; Wakabayashi, 1992, 1999). This distinction is important in distinguishing the different types of metamorphic rocks in the Franciscan Complex and their significance. Metamorphism in coherent terranes ranges from zeolite facies to blueschist-greenschist transition facies (Blake et al., 1988), whereas tectonic blocks include rocks with the same metamorphic grade as the coherent terranes in addition to high-grade blocks that exhibit eclogite and amphibolite assemblages (Coleman and Lanphere, 1971). Many, if not most, high-grade blueschist and eclogite blocks have relics of earlier amphibolite-grade metamorphic assemblages (Moore and Blake, 1989; Wakabayashi, 1990). High-grade blocks are entirely metabasites with minor metacherts, whereas coherent metamorphic rocks are mostly metagraywackes and metashales, with lesser proportions of metabasites and metacherts (Blake et al., 1988; Coleman and Lanphere, 1971). Many high-grade blocks are partly encased in "rinds" composed of minerals such as actinolite, chlorite, talc, and phengite: this rind apparently formed by metasomatic reaction between the block and the ultramafic rocks (e.g., Coleman and Lanphere, 1971; Moore, 1984). High-grade block metamorphism evolved along a counterclockwise *P-T* path (P on the positive *y*-axis; Wakabayashi, 1990), whereas metamorphism in coherent metamorphic rocks took place under a mildly clockwise or hairpin *P-T* trajectory (Maruyama and Liou, 1988; Maruyama et al., 1985).

The high-grade blocks are the oldest metamorphic rocks in the Franciscan, and the age of their high-temperature metamorphism is 153–169 Ma (Ross and Sharp, 1988; Catlos and Sorensen, 2003; Anczkiewicz et al., 2004). The ages of blueschist metamorphism in the blocks range from 138 to 159 Ma, whereas the ages of coherent blueschist metamorphism range from 145 to 80 Ma (Wakabayashi, 1999). Peak temperatures of Franciscan metamorphism decrease with decreasing age from amphibolite temperatures of >600 °C in the high-grade blocks (Wakabayashi, 1990) at 159–169 Ma (Ross and Sharp, 1988; Anczkiewicz et al., 2004), to 300–350 °C for blueschist-greenschist–grade rocks (Blake et al., 1988; Maruyama and Liou, 1988) at ca. 145 Ma (Wakabayashi and Deino, 1989), to 150–250 °C for lawsonite-bearing blueschist facies rocks (Ernst, 1971a; Maruyama et al., 1985) at 80–120 Ma (Wakabayashi, 1999), and ultimately to zeolite and prehnite-pumpellyite temperatures of <200 °C (Blake et al., 1988) for the last 80 m.y. (Wakabayashi, 1999). Peak metamorphic pressures of exposed Franciscan rocks are similar for high-grade blocks and blueschist facies rocks and range from ~6 to 14 kbar (Maruyama et al., 1985;Wakabayashi, 1990; Giaramita and Sorensen, 1994; Anczkiewicz et al., 2004), whereas sub-blueschist-grade rocks were metamorphosed at pressures <4 kbar (Blake et al., 1988).

Metamorphic ages of Franciscan rocks approximate the time of subduction, because exhumation of these rocks occurred while subduction and refrigeration were ongoing; the only process that could cause metamorphic ages to depart significantly from subduction ages is late heating that did not occur in the Franciscan (Ernst, 1988). The high-grade blocks have been suggested to represent rocks formed at the inception of subduction beneath hot suboceanic upper mantle material on the basis of their old age, lithology, presence of rinds, and *P-T* evolution (Wakabayashi, 1990), whereas lower grade Franciscan rocks formed during subsequent subduction. Recently obtained Lu-Hf ages from high-grade blocks are interpreted as metamorphic crystallization rather than cooling ages of the blocks (Anczkiewicz et al., 2004). These ages of amphibolite or eclogite metamorphism from high-grade blocks are 153 ± 0.4 Ma from a garnet amphibolite from Ring Mountain, 157.9 ± 0.7 Ma from an eclogite from Jenner, 162.5 ± 0.5 Ma from a garnet amphibolite block from El Cerrito, and 168.7 ± 0.8 Ma from a garnet amphibolite from Panoche Pass. These ages are consistent with $^{40}Ar/^{39}Ar$ hornblende ages from high-grade blocks that range in age from 158 to 163 Ma (Ross and Sharp, 1986, 1988) and may represent either crystallization or cooling ages, depending on the sample. The age of high-temperature metamorphism in the high-grade blocks is slightly younger than the crystallization age of the 165–172 Ma Coast Range Ophiolite and associated rocks (Shervais et al., 2005; Hanan et al., 1992; Hopson et al., 1996; Mattinson and Hopson, 1992), indicating that the ophiolite was young and hot at the time Franciscan subduction began tectonically beneath it.

The pronounced cooling between the peak temperature of high-grade block metamorphism and the peak temperature of blueschist-greenschist metamorphism probably indicates cooling as subduction proceeded; the cooling was a consequence of (1) refrigeration of the hanging wall by continued subduction, and (2) subduction of progressively older and cooler oceanic crust (Cloos, 1985; Platt, 1975). The blueschist-greenschist–grade rocks appear to exhibit a slightly clockwise *P-T* path in contrast to the counterclockwise *P-T* path of the high-grade blocks (Wakabayashi, 1999). This difference probably is also a consequence of the refrigeration of the hanging wall and the subduction of older, cooler crust (Wakabayashi, 1999).

Geochemical data from coherent volcanic rocks of the Franciscan suggest that these rocks are predominantly OIB, with some rocks of MORB chemistry (MacPherson et al., 1990; Shervais, 1990; Shervais and Kimbrough, 1987), whereas fine-grained blueschist and lower-grade tectonic blocks include OIB, MORB, and island-arc chemistry (MacPherson

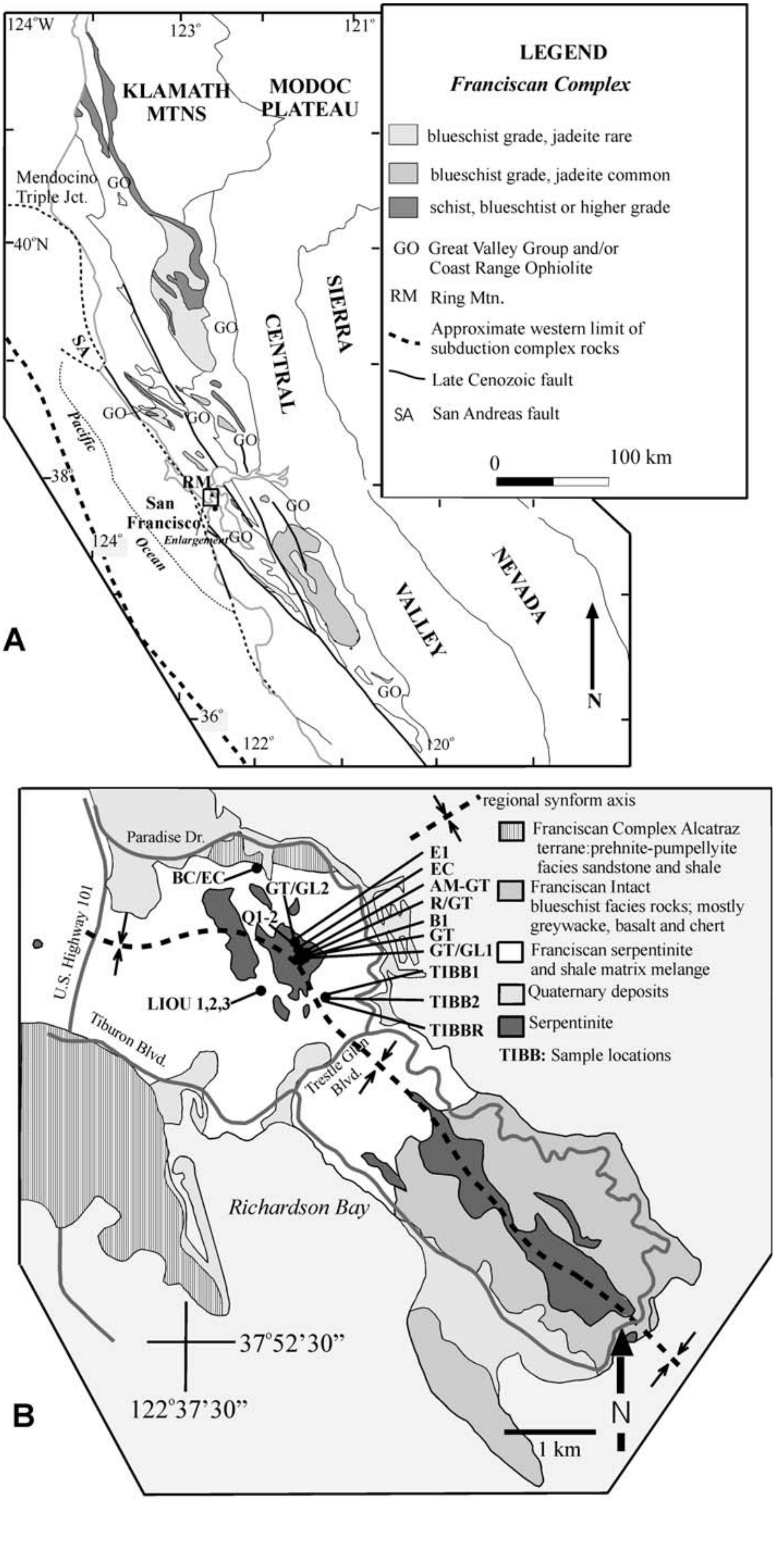

Figure 1. (A) Distribution of Franciscan and basement rocks of central and northern California, showing Franciscan rocks, of different metamorphic grades. Map derived from various sources and compiled from Wakabayashi (1999). Ring Mountain high-grade tectonic block locality is shown as (RM). (B) Sample localities of this study are shown on this map. Brief petrographic descriptions of these samples are given in the Appendix. Geochemical results of rocks from the Ring Mountain locality are presented and discussed in this paper.

et al., 1990). A recent study (Swanson et al., 2004) of blueschist-greenschist–grade metabasaltic rocks from Ward Creek, a unit that may have been accreted at or before ca. 145 Ma, interpreted island-arc chemistry for their protolith. With the exception of Ward Creek, rocks that have been analyzed in previous studies may have been subducted at ca. 90–100 Ma, on the basis of fossil ages (ca. 100 Ma) from graywackes that overlie them within their respective terranes; volcanic rocks appear to have been accreted at other times in Franciscan history, but their geochemistry has not been examined in detail. Most volcanic rocks within the Franciscan have estimated formational ages that are much older than the age at which they were subducted, indicating that the ocean crust from which they were derived was old at the time of its arrival at the Franciscan trench and had traveled thousands of kilometers from its site of formation to the trench (Wakabayashi, 1999). In contrast to most of the volcanic rocks in the Franciscan, the Coast Range Ophiolite exhibits island-arc chemistry and is thought to represent the early stages of arc development (Giaramita et al., 1998; Shervais, 2001).

SAMPLE LOCATIONS

High-grade blocks analyzed in this study were collected from a serpentinite and shale matrix mélange from Ring Mountain on Tiburon Peninsula in the San Francisco Bay region (Fig. 1A, 1B). This mélange is the structurally highest of the series of Franciscan nappes in the region (Wakabayashi, 1992). A variety of block types occur at Ring Mountain, including garnet amphibolites, epidote amphibolites, eclogites, and blueschists, and corresponding peak metamorphic temperatures and pressures also vary widely from block to block. All the blocks are metabasites and metacherts. No high-grade metagraywackes or metashales have been found. Metabasites probably are primarily metabasalts rather than metagabbros, because metachert layers are common within metabasite blocks. In other words, the block protoliths represent the very top layer of subducted oceanic crust. Thermobarometry has been conducted on one of the blocks sampled (the TIBB sample is the same TIBB sample of Wakabayashi, 1990); thermobarometry has also been conducted on additional blocks at Ring Mountain that are similar to the other blocks sampled (Giaramita and Sorensen, 1994; Wakabayashi, 1990).

In addition to the regionwide geochronologic data on high-grade blocks just reviewed, detailed geochronologic information was obtained from high-grade blocks at Ring Mountain. Spot $^{40}Ar/^{39}Ar$ dates on phengites from garnet amphibolite and eclogite (range, 151.6 ± 4.1–157.5 ± 1.8 Ma), block rind (range, 141.0 ± 1.7–160.6 ± 3.3 Ma), and a phengite chlorite vein (range, 150.2 ± 1.1–160.3 ± 5.2 Ma) represent a total of 37 dates (Catlos and Sorensen, 2003).

The geochemical results of our detailed study of Franciscan blueschists and eclogites, as described later, are significant in this context. Sample locations are shown in Figure 1B, whereas brief descriptions of the petrography, as well as locations of the samples, are given in the Appendix.

ANALYTICAL METHODS

For this study, 16 samples of blueschist, eclogite, actinolite rind, and garnet amphibolite from the tectonic blocks of the Franciscan Complex were analyzed for major element and trace element concentrations and Sr, Nd, and Pb isotopic systematics. Samples were powdered, using an agate ball mill. Trace elements were determined by an inductively coupled plasma–mass spectrometer (ICP-MS PQ II+), whereas radiogenic isotopic ratios were measured with a thermal-ionization mass spectrometer (TIMS VG Sector), both at the University of Rochester.

Major elements were analyzed in a commercial laboratory—Actlabs, in Ontario, Canada. The samples underwent lithium metaborate/tetraborate fusion, followed by measurement on an ICP-OES (optical emission spectrometry). Repeated measurements of known rock standards indicate that the concentrations of the major elements are within 0.1% and are also certified as such by the laboratory. Zr measurements were from the ICP-OES. For the ICP-MS analyses in our laboratory, 100 mg powdered digested samples were diluted to 100 mL of 5% HNO_3 solution with ~10 ppb internal standard of In, Cs, Re, and Bi. The concentrations were obtained by using BCR-2 and BIR-2 (concentrations from the U.S. Geological Survey) as known standards. The concentrations of the various elements are within a 5% error, based on repeated measurements of SRM 278 (obsidian, U.S. National Institute of Standards and Technology) and BHVO-2 (basalt, U.S. Geological Survey), which were run as unknowns. Nb and Hf measurements were done by neutron activation analysis at Oregon State University. Data are given in Table 1.

Nd and Sr isotopes were measured with a VG Sector multi-collector TIMS, using the procedures established for our laboratory at the University of Rochester (Basu et al., 1990); Pb isotopes were also measured with the procedure established later (Sharma et al., 1992). The filament temperature during Pb isotope ratio measurements was monitored continuously, and raw ratios were calculated as weighted averages of the ratios measured at 1150 °C, 1200 °C, and 1250 °C, respectively. The reported Pb isotopic data are corrected for mass fractionation of 0.12 ± 0.03% per atomic mass unit, based on replicate analyses of the NBS-982 equal atom Pb standard measured in the same fashion. Our laboratory procedural blanks were <400 pg (picogram) for Sr and <200 pg for both Nd and Pb. No blank correction was necessary for the data in Table 2.

GEOCHEMICAL TRACER RESULTS FOR FRANCISCAN HIGH-GRADE BLOCKS

The analytical results of the samples are shown in Tables 1 and 2 and in Figures 2–6. Some of the tectonic and petrogenetic implications of these results are summarized in the cross-sectional cartoons of Figure 7. In examining the bulk-rock geochemical data, we classify these samples from petrographic observations into blueschists, actinolite-bearing rinds, eclogites, and garnet amphibolites, realizing that titanite and rutile are part of the stable mineral assemblages in these rocks and may control some key trace element distributions (Manning and Bohlen, 1991; Ryerson and Watson, 1987). In the following sections we present the data for the rocks studied. The garnet amphibolites, eclogites, and blueschists, or collectively the high-grade blocks, are discussed in a separate section from that of the actinolite rinds. Following this, we conclude that the geochemical patterns are not an artifact of chemical changes caused by metamorphism but are the original signature of the rocks.

High-Grade Blocks: Blueschists, Eclogites, and Garnet Amphibolites

Geochemical Data

Major element data for the high-grade rocks are given in Table 1. SiO_2 (wt%) and Na_2O + K_2O (wt%) of the 13 samples can be compared with those from some Coast Range Ophiolite rocks (Shervais, 1990) and N-MORB from the East Pacific Rise (from the PETDB database, compiled by the Lamont-Doherty Earth Observatory), and various volcanic rocks from the Mariana arc (from the GEOROC database, compiled by the Max Planck Institute). Although the SiO_2 contents of these samples vary between ~42 and 56 wt%, and the Na_2O + K_2O contents fall between ~1.6 and 6.1 wt%, making the protoliths of these rocks comparable to non-MORB–type basaltic rocks of orogenic belts, this comparison may be inappropriate because of possible seafloor alteration. Rocks

TABLE 1. MAJOR ELEMENT AND TRACE ELEMENT CONCENTRATIONS OF THE FRANCISCAN HIGH-GRADE ROCKS FROM THE RING MOUNTAIN TECTONIC BLOCK

Sample	LIOU 1	LIOU 2	LIOU 3	B 1	AM/GT	GT	GT/GL(1)	R/GT	EC	E1	GT/GL(2)	Q1	BC/EC	TIBB-2	TIBB	TIBB-R
Rock type	blueschist	Blueschist	blueschist	blueschist	gt. amp.	gt. amp.	rind ?	rind	eclogite	eclogite	gt. amp.	gt. amp.	eclogite	blueschist	gt. amp.	rind
SiO_2	50.70	52.13	51.08	49.90	44.24	42.91	50.63	55.73	47.16	45.72	47.27	53.29	51.46	48.22	42.75	46.45
Al_2O_3	12.08	11.10	12.25	17.41	14.06	16.10	8.93	3.02	16.71	17.63	15.38	11.77	12.28	14.56	15.94	15.83
FeO	11.93	11.89	11.40	8.83	12.44	10.92	7.95	6.21	6.33	7.19	11.04	9.68	9.89	9.98	12.01	9.04
MnO	0.15	0.17	0.17	0.09	0.28	0.21	0.21	0.23	0.10	0.12	0.19	0.28	0.22	0.16	0.27	0.16
MgO	8.13	9.26	8.36	5.93	9.59	7.48	16.45	19.59	6.31	7.13	5.21	10.16	6.92	9.38	9.35	12.88
CaO	2.98	2.43	2.97	5.61	5.53	14.01	8.98	10.64	13.06	14.24	12.47	6.14	11.02	3.19	10.93	5.03
Na_2O	4.87	5.44	4.39	4.19	3.52	1.43	2.47	1.43	3.49	3.18	1.83	3.25	4.84	3.30	2.68	2.55
K_2O	0.83	0.54	1.41	0.91	0.77	0.33	0.22	0.22	1.36	0.54	0.16	1.86	0.88	2.80	0.42	2.58
TiO_2	2.26	2.15	2.19	0.69	1.58	2.75	0.30	0.05	0.96	1.28	2.34	0.72	1.45	0.52	0.84	0.45
P_2O_5	0.25	0.20	0.20	0.02	0.03	0.18	-0.01	0.01	0.13	0.12	0.20	0.11	0.11	0.06	-0.01	-0.01
LOI	3.21	2.67	3.62	4.70	5.18	1.97	2.04	1.90	2.27	2.31	1.55	1.75	0.29	6.21	2.05	3.62
Total	98.72	99.31	99.29	99.26	98.59	99.50	99.07	99.73	98.57	100.26	98.86	100.07	100.40	99.49	98.58	99.58
Rb	22.9	10.4	30.8	19.8	23.6	8.2	1.4	3.9	35.6	20.1	2.3	38.6	15.1	110.1	5.9	54.8
Ba	424.8	226.3	699.8	417.5	534.6	127.6	46.1	84.7	1405.2	784.7	22.2	911.6	326.7	1589.0	121.6	1474.9
Sr	41.6	17.6	29.3	169.3	230.1	511.6	13.0	14.4	376.5	382.6	104.7	48.8	39.9	392.4	246.8	44.4
Pb	27.5	12.0	7.5	3.1	6.4	14.9	3.1	2.3	7.1	6.7	2.7	1.7	1.3	1.0	10.3	2.6
La	3.8	5.0	5.0	2.0	5.0	13.1	0.8	0.1	7.9	6.9	9.8	7.8	7.6	3.7	6.0	0.7
Ce	11.9	15.4	15.7	4.3	14.6	33.1	1.7	0.4	17.4	15.6	25.9	13.8	21.5	6.4	14.2	2.4
Pr	2.1	2.7	2.8	0.9	2.5	5.0	0.3	0.1	2.4	2.2	4.1	2.1	3.6	1.2	2.2	0.3
Nd	10.7	13.7	14.4	5.0	13.2	23.3	1.3	0.7	10.2	9.6	19.3	8.9	17.6	5.8	10.7	1.5
Sm	3.6	4.5	5.1	2.1	4.8	7.5	0.4	0.3	3.4	3.0	5.9	2.8	5.7	2.2	3.4	1.0
Eu	1.2	1.4	1.8	0.8	2.0	2.7	0.1	0.1	1.4	1.1	2.0	1.1	1.8	1.0	1.1	0.5
Gd	4.0	5.1	6.2	3.1	6.3	9.3	0.6	0.4	3.4	3.0	7.4	3.4	6.8	2.5	4.3	1.0
Tb	0.7	1.0	1.2	0.5	1.2	1.7	0.1	0.1	0.6	0.5	1.4	0.7	1.1	0.4	0.8	0.2
Dy	4.4	6.2	7.3	3.3	7.5	10.7	0.9	0.7	3.8	3.4	8.5	4.0	5.9	2.9	5.2	1.4
Ho	0.9	1.4	1.6	0.8	1.7	2.3	0.2	0.1	0.8	0.7	1.8	0.7	1.3	0.7	1.1	0.3
Er	2.4	3.9	4.8	2.1	5.0	6.5	0.6	0.5	2.3	2.0	5.2	1.7	3.9	2.0	3.5	1.1
Tm	0.4	0.6	0.7	0.3	0.7	0.9	0.1	0.1	0.3	0.3	0.7	0.2	0.6	0.3	0.5	0.2
Yb	2.3	3.9	4.5	1.4	4.8	5.8	0.6	0.5	2.1	1.9	4.7	1.4	4.2	1.9	3.3	1.2
Lu	0.3	0.5	0.6	0.2	0.7	0.8	0.1	0.1	0.3	0.3	0.7	0.2	0.6	0.3	0.5	0.2
Y	23.9	35.2	40.6	21.5	46.4	68.7	5.1	4.4	23.1	20.4	44.3	18.7	39.6	21.0	27.8	9.9
Th	0.4	0.3	0.2	0.2	0.3	1.2	0.2	0.0	0.9	1.0	0.9	0.9	0.4	0.4	0.9	0.4
U	0.2	0.2	0.1	0.3	0.4	0.8	0.0	0.0	0.2	0.2	0.5	0.5	0.5	0.2	0.7	0.1
Zr	127.0	122.0	127.0	30.0	93.0	151.0	23.0	2.0	62.0	86.0	143.0	53.0	96.0	37.0	71.0	15.0
Hf	4.1	3.9	4.0	12.0	3.0	4.9	0.8	0.2	1.8	2.2	3.9	2.3	2.9	1.3	2.1	0.9
Nb	3.9	3.8	3.3	1.1	3.9	12.8	0.5	0.0	11.5	12.0	9.0	1.3	5.3	0.8	3.2	1.0

Notes: Major elements were measured by ICP-OES (inductively coupled plasma–optical emission spectrometry), concentrations are in wt%, and analytical uncertainties are 0.01%. The trace elements were measured by ICP-MS (inductively coupled plasma–mass spectrometer), all the concentrations are in ppm (μg/g), and analytical uncertainties are within 5%. Nb and Hf values were obtained by INAA (instrumental neutron activation analysis) at Oregon State University, with similar uncertainties. Samples are grouped according to tectonic blocks from which they were collected. Rock type is also shown; gt. amp.—garnet amphibolite.

TABLE 2. Rb-Sr, Sm-Nd, AND U-Th-Pb ISOTOPIC DATA OF THE FRANCISCAN HIGH-GRADE BLOCKS

Sample	LIOU-1	LIOU-2	LIOU-3	TIBB-2	TIBB	TIBB-R	B-1	AM/GT	GT	GT/GL-1	R/GT	EC	E1	GT/GL-2	Q1–2	BC/EC
Sm (ppm)†	3.58	4.51	4.86	2.21	3.35	0.97	2.14	4.71	7.51	0.45	0.34	3.39	2.96	5.79	2.84	5.64
Nd (ppm)†	10.68	13.72	13.76	5.81	10.47	1.48	4.96	12.92	23.35	1.27	0.70	10.22	9.65	18.96	8.91	17.31
$^{147}Sm/^{144}Nd$	0.212	0.208	0.223	0.241	0.202	0.414	0.272	0.231	0.203	0.223	0.304	0.210	0.194	0.193	0.202	0.206
$^{143}Nd/^{144}Nd_{(measured)}$ ‡	0.513061	0.513052	0.512942	0.512919	0.512957	0.512915	0.513149	0.513165	0.513058	0.512773	0.512992	0.512969	0.512970	0.513019	0.512695	0.513044
2 s.e.§	21	33	22	27	39	29	87	31	21	20	37	23	18	32	33	17
$\varepsilon_{Nd\ (at\ 170\ Ma)}$ #	**7.9**	**7.8**	**5.3**	**4.5**	**6.1**	**1.2**	**8.4**	**9.5**	**8.0**	**2.0**	**4.7**	**6.1**	**6.5**	**7.5**	**1.0**	**7.7**
Rb (ppm)†	22.86	10.36	30.83	110.15	5.88	54.78	19.76	23.59	8.18	1.43	3.93	35.59	20.09	2.27	38.64	15.07
Sr (ppm)†	41.56	17.62	29.26	392.38	246.81	44.38	169.33	230.11	511.55	12.98	14.40	376.53	382.57	104.69	48.78	39.92
$^{87}Rb/^{86}Sr$	1.555	1.662	2.978	0.794	0.067	3.489	0.330	0.290	0.045	0.312	0.772	0.267	0.148	0.061	2.240	1.067
$^{87}Sr/^{86}Sr_{(measured)}$ ††	0.707619	0.708702	N.D.	0.706862	0.705032	0.713098	0.705242	0.705723	0.705385	0.709205	0.708047	0.705477	0.705102	0.704511	0.710820	0.706897
2 s.e.‡‡	31	33	N.A.	35	32	60	32	30	27	35	20	35	49	38	47	38
$^{87}Sr/^{86}Sr_{(at\ 170\ Ma)}$	**0.70408**	**0.70492**	**N.A.**	**0.70506**	**0.70488**	**0.70516**	**0.70449**	**0.70506**	**0.70428**	**0.70849**	**0.70629**	**0.70487**	**0.70476**	**0.70437**	**0.70573**	**0.70447**
Pb (ppm)†	27.48	12.02	7.51	0.97	10.25	2.57	3.09	6.40	14.92	3.13	2.32	7.12	6.72	2.70	1.70	1.26
Th (ppm)†	0.43	0.25	0.20	0.41	0.93	0.39	0.24	0.31	1.20	0.20	0.03	0.91	1.03	0.93	0.93	0.39
U (ppm)†	0.23	0.17	0.15	0.23	0.73	0.09	0.29	0.43	0.82	0.02	0.01	0.23	0.23	0.47	0.50	0.53
$^{206}Pb/^{204}Pb_{(measured)}$ §§	18.144	18.316	18.269	18.826	18.479	18.485	18.488	18.442	18.436	18.381	18.251	18.402	18.398	18.448	18.864	18.837
2 s.e.##	4	3	5	8	6	8	4	7	3	4	6	6	5	5	5	5
$^{207}Pb/^{204}Pb_{(measured)}$ §§	15.475	15.462	15.458	15.519	15.456	15.468	15.470	15.507	15.475	15.505	15.517	15.472	15.467	15.459	15.513	15.460
2 s.e.##	4	3	5	7	5	11	3	6	2	4	6	6	5	5	4	5
$^{208}Pb/^{204}Pb_{(measured)}$ §§	37.590	37.774	37.667	38.220	37.895	38.016	37.855	37.966	37.913	37.870	37.844	37.925	37.918	37.834	38.265	37.799
2 s.e.†††	10	06	14	18	14	19	08	16	06	09	17	18	13	15	11	12
($^{238}U/^{204}Pb$)	0.52	0.88	1.25	15.23	4.46	2.16	5.95	4.25	3.44	0.42	0.38	2.01	2.16	10.99	18.89	26.64
($^{235}U/^{204}Pb$)	0.0038	0.0064	0.0090	0.1105	0.0323	0.0156	0.0431	0.0308	0.0249	0.0031	0.0027	0.0146	0.0157	0.0797	0.1370	0.1932
($^{232}Th/^{204}Pb$)	1.00	1.36	1.71	28.07	5.91	9.86	4.96	3.14	5.22	4.16	0.81	8.38	9.96	22.42	36.00	20.07
$^{206}Pb/^{204}Pb_{(initial\ at\ 170Ma)}$	**18.13**	**18.29**	**18.24**	**18.44**	**18.37**	**18.43**	**18.34**	**18.33**	**18.35**	**18.37**	**18.24**	**18.35**	**18.34**	**18.17**	**18.39**	**18.17**
$^{207}Pb/^{204}Pb_{(initial\ at\ 170Ma)}$	**15.47**	**15.46**	**15.46**	**15.50**	**15.45**	**15.47**	**15.46**	**15.50**	**15.47**	**15.50**	**15.52**	**15.47**	**15.46**	**15.45**	**15.49**	**15.43**
$^{208}Pb/^{204}Pb_{(initial\ at\ 170Ma)}$	**37.58**	**37.75**	**37.64**	**37.79**	**37.80**	**37.87**	**37.78**	**37.92**	**37.83**	**37.81**	**37.83**	**37.80**	**37.77**	**37.49**	**37.72**	**37.49**

†Rb, Sr, Sm, Nd, U, Th, and Pb concentration were measured on the ICP-MS (inductively coupled plasma–mass spectrometer), and analytical uncertainties are 5%. Isotopic ratios of Nd, Sr, and Pb were measured on TIMS (thermal ionization mass spectrometer).

‡Measured $^{143}Nd/^{144}Nd$ ratios normalized to $^{146}Nd/^{144}Nd = 0.7219$. La Jolla Nd standard analyzed during the course of this study yielded $^{143}Nd/^{144}Nd = 0.511854+24$ (2σ) ($n = 5$).

§Two standard errors corresponding to the 5th decimal place.

#Calculated using present-day bulk-earth value of $^{143}Nd/^{144}Nd = 0.512638$ and $^{147}Sm/^{144}Nd = 0.1967$.

††Measured $^{87}Sr/^{86}Sr$ ratio normalized to $^{86}Sr/^{88}Sr = 0.1194$. NBS-987 Sr standard analyzed during the course of this study yielded $^{87}Sr/^{86}Sr = 0.710234+23$ (2σ) ($n = 6$).

‡‡Two standard errors corresponding to the 5th decimal place.

§§For Pb isotopic analyses, mass fractionation was monitored by analysis of the NBS-981 Pb standard and was typically ~0.12% per a.m.u. (atomic mass unit).

##Two standard errors corresponding to the 3rd decimal place.

†††Two standard errors corresponding to the 2nd decimal place.

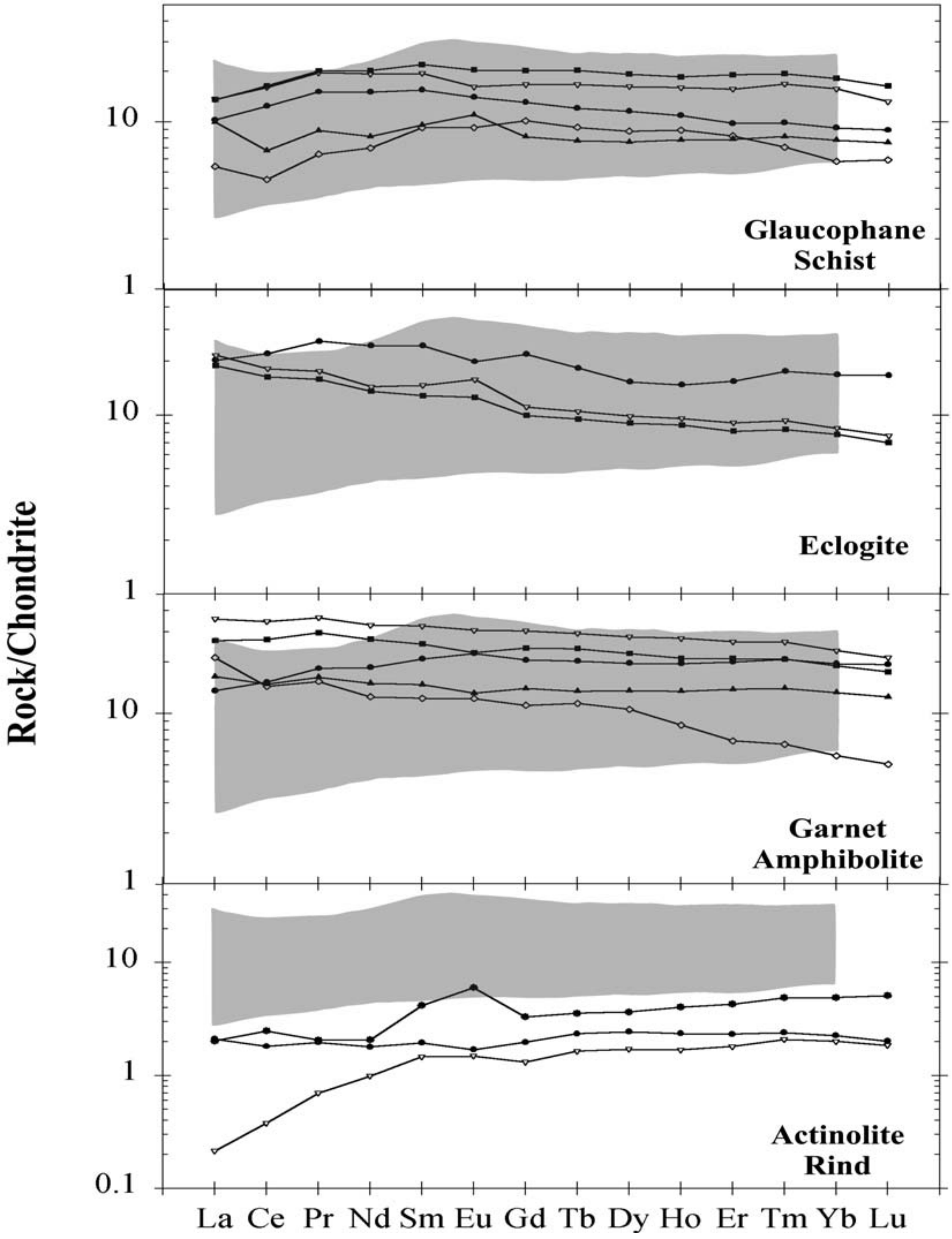

Figure 2. Chondrite-normalized rare earth element (REE) patterns of five blueschists, three eclogites, five garnet amphibolites, and three actinolite rinds of the Ring Mountain tectonic block of this study. This group of rocks, with the exception of the actinolite rinds, displays broadly similar, generally flat patterns, with most of the blueschists and a garnet amphibolite showing slight light REE depletion analogous to South Sandwich Islands, Izu-Bonin, and Mariana arc basalts (Tatsumi and Eggins, 1995; Hawkesworth et al., 1977). Overall, these REE patterns are similar to global arc basalts, especially trench-side basalts. The shaded region, for comparison, shows the general range of Western Pacific arc tholeiite data (Jakes and Gill, 1970).

of the Coast Range Ophiolite, parts of which are believed to have formed in an arc setting, show similar chemical variations as those of the high-grade samples of this study. FeO*/MgO ratios (where FeO* is total Fe as FeO), when compared against TiO_2 (wt%) of the high-grade blocks (not shown here), show restricted values of FeO*/MgO from 0.95 to 1.2, whereas TiO_2 values vary from 0.52 to 2.75 wt%. Shervais and Kimbrough (1985) use this variation to define fields for the northern and southern Coast Range Ophiolite on the basis of the slopes of the observed trends. The Franciscan high-grade-block data indicate both arc-tholeiite–like and MORB-like major element chemistry, according to their TiO_2 and FeO*/MgO variations, following the Coast Range Ophiolite–defined criteria. However, we consider this variation nondiagnostic because fO_2 variations during arc magma generation in the subduction environment also may be responsible for these trends. Thus, major element chemical variations are not diagnostic for the purpose of protolith characterization.

Chondrite-normalized REE patterns for the high-grade blocks are shown in the upper three panels of Figure 2. The REE patterns of the high-grade rocks show relatively flat patterns, with distinct depletions in La and Ce, and the concentrations vary between 5 and 40 times chondritic. Blueschists show light rare earth element (LREE) depletions with $(La/Sm)_n$ values of ~0.6 and $(Gd/Lu)_n$ values of ~1.5, with the exception of sample TIBB-2, which gives a value of 1 for both the ratios. Eclogites and garnet amphibolites generally show slight LREE-enriched patterns (except for sample AM/GT), with $(La/Sm)_n$ between 0.7 and 1.5, and $(Gd/Lu)_n$ between ~1.1 and 2.2. The overall REE patterns are similar to those of arc basalts, such as those from the South Sandwich Islands and the Marianas (Hawkesworth et al., 1977; Tatsumi and Eggins, 1995), and are distinctly different from OIB. For a broad comparison, the Western Pacific arc tholeiite REE data (Jakes and Gill, 1970) are shown by the shaded regions in Figure 2. The blueschist, eclogite, and garnet amphibolite data overlap the Western Pacific arc tholeiite REE data.

Rb-Sr and Sm-Nd isotopic data are given in Table 2. The initial ε_{Nd} at 170 Ma, which approximates the older ages of formation of the Coast Range Ophiolite (Shervais et al., 2005; Hanan et al., 1992; Hopson et al., 1996; Mattinson and Hopson, 1992) clusters between +4.5 and +9.5 for the high-grade blocks. Initial $^{87}Sr/^{86}Sr$ data at 170 Ma range from 0.70408 to 0.70506. The initial ε_{Nd} and $^{87}Sr/^{86}Sr$ of these rocks are plotted in Figure 3 along with the fields for MORB, arc tholeiites, oceanic sediments, and upper Middle Jurassic Sr isotopic composition of seawater. The initial ε_{Nd} values at 170 Ma of all the samples studied fall outside the present-day MORB field (Fig. 3).

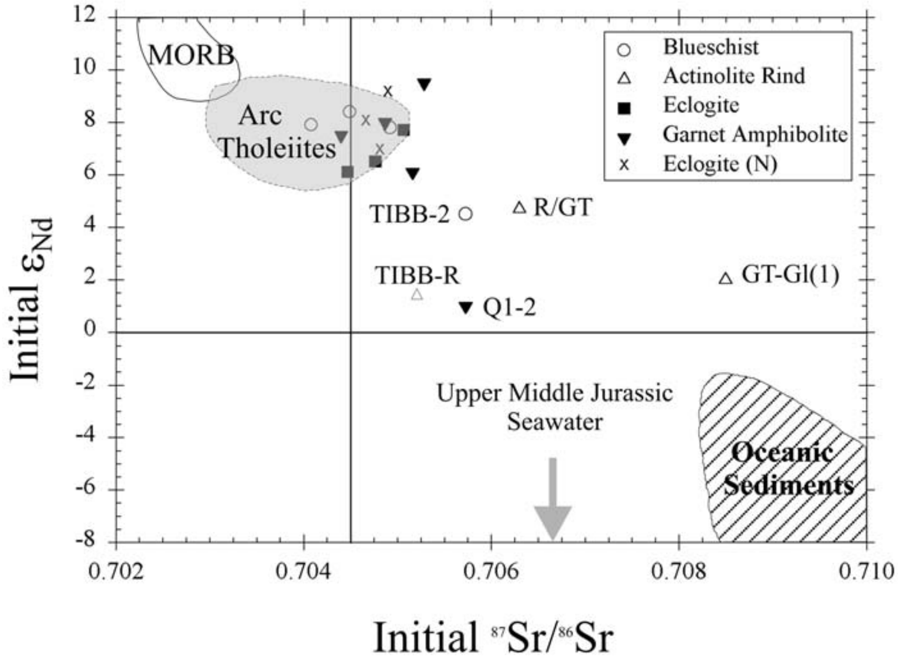

Figure 3. Initial $^{87}Sr/^{86}Sr$ and ε_{Nd} values at 170 Ma in the Franciscan high-grade rocks of this study, compared with fields for present-day mid-oceanic-ridge basalt (MORB), global arc tholeiites, and part of the field for oceanic sediments (Tatsumi and Eggins, 1995). Most of the samples, with the exception of five samples, especially the actinolite rinds, fall in the arc tholeiite field. The characteristic isotopic signatures of these five samples are discussed in the text, including the presence of metacherts in some of these high-grade rocks. Eclogites analyzed from a previous study (Nelson, 1995) fall close to the eclogites analyzed in this study. The composition of late Middle Jurassic seawater and the general field of oceanic sediments are shown for reference (from literature).

Pb isotopic ratios of Franciscan high-grade blocks of this study are reported in Table 2 and are plotted in Figure 4. Initial $^{206}Pb/^{204}Pb$ and $^{207}Pb/^{204}Pb$ values at 170 Ma range from 18.13–18.44 to 15.43–15.52, respectively. Initial $^{208}Pb/^{204}Pb$ values range from 37.49 to 37.92. Their initial ratios in plots of $^{207}Pb/^{204}Pb$ and $^{208}Pb/^{204}Pb$ against $^{206}Pb/^{204}Pb$ at 170 Ma are illustrated in Figure 4. These data are compared with the present-day Pb isotope ratios of basaltic and andesitic rocks of three intra-oceanic arcs—the Mariana, Kurile, and Izu-Bonin arcs of the Western Pacific (from the GEOROC database, compiled by the Max Planck Institute). For reference, various mantle reservoirs and the Northern Hemisphere Reference Line (NHRL) for Pb isotopes in oceanic basalts are shown in Figure 4. Even though the Franciscan Pb data are similar to Pacific MORB (Church and Tatsumoto, 1975; Hanan and Schilling, 1989; Tatsumoto, 1978; White et al., 1987), they show a similarity to the Izu-Bonin arc (Pearce et al., 1992). A combined $^{206}Pb/^{204}Pb$, $^{207}Pb/^{204}Pb$, and $^{208}Pb/^{204}Pb$ plot of the Franciscan rocks in Figure 4 shows that the high-grade blocks are distinct from continental crustal values, inasmuch as they are restricted to the oceanic basalt field near the NHRL. The Mariana arc shows an overall trend steeper than the NHRL. Samples with lower $^{206}Pb/^{204}Pb$ values fall close to the NHRL, as also seen in some Oligocene Izu-Bonin volcanics (Pearce et al., 1992) and in the Franciscan samples. Also shown in Figure 4 for comparison is the field of the only published Pb isotopic data from the Coastal Range Ophiolite (Hanan et al., 1991). This ophiolite plots close to the Franciscan rocks of this study.

On a Ce/Pb versus Ce concentration plot (Fig. 5) the samples under discussion have Ce concentrations from 4.3 to 33.1 ppm, and Ce/Pb varies from 0.4 to 2.4 with the exception of blueschist (TIBB-2) and an eclogite (BC/EC), which have Ce/Pb >6 (Table 1; Fig. 5). The Franciscan data are compared in Figure 5 with the global reservoirs of MORB, OIB, average continental crust, bulk-earth composition, and the field for global arc basalts.

The Nb/U ratio in global reservoirs also follows the same pattern as that for Ce/Pb (Hofmann

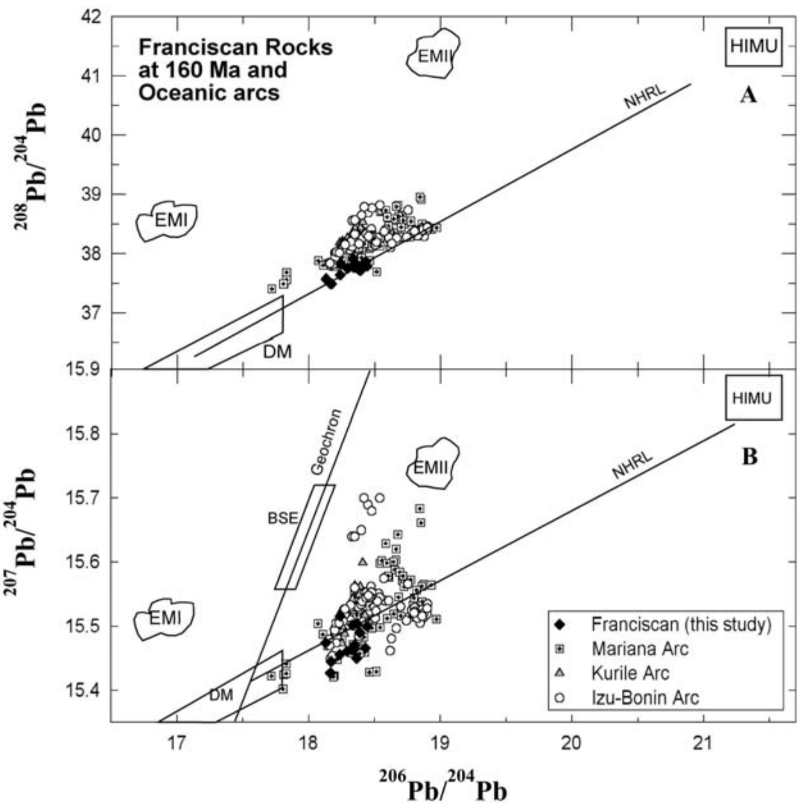

Figure 4. Initial Pb isotopic compositions at 170 Ma of the Franciscan high-grade rocks of this study in comparison with present-day Pb isotopic ratios of basaltic and andesitic rocks of three intra-oceanic arcs of the Western Pacific. These arc data are from previous studies as compiled by the Max Planck Data Sources. The Franciscan Pb isotopic ratios, although similar to Pacific MORB (Church and Tatsumoto, 1975; Hanan and Schilling, 1989; Tatsumoto, 1978; White et al., 1987), are most remarkably similar to the frontal-arc lavas of the Izu-Bonin arc. To make a valid comparison with the present-day Pb data of the arc lavas, note that after 170 m.y. of evolution, the Franciscan Pb data should lie slightly to the right along the Northern Hemisphere Reference Line (NHRL), but still far removed from possible continental crustal contamination, especially with respect to $^{207}Pb/^{204}Pb$. Also shown for comparison is the field of Pb isotopic data from the Coast Range Ophiolite (Hanan et al., 1991). CRO—Coast Range Ophiolite; EM—enriched mantle; BSE—bulk silicate earth; HIMU—high $^{238}U/^{204}Pb$ ratio.

et al., 1986); Nb is deficient in continental crust and subduction-related lavas (Briqueu et al., 1984). Nb concentrations in the samples vary between 0.03 and 12.8 ppm (Table 1). With the exception of two eclogites (E1, EG), Franciscan rocks show low Nb/U ratios, ranging from 2.5 to 23 (compared to a mantle Nb/U = 47 ± 10), indicating depletion in Nb compared to U. Similarly, Nb/La ratios in the Franciscan samples are generally lower than MORB value (Nb/La = 0.9), varying between 0.3 and 1.3.

Other incompatible and compatible trace element patterns, including the REE of the high-grade blocks, are shown in Figure 6, normalized to N-MORB. The high-grade blocks are shown in the first three panels of Figure 6. All the samples show prominent LILE enrichment. Pb also shows enrichment, as observed in Figure 5. Nb depletion is prominent for certain blueschists and garnet amphibolites of this study.

Discussion

Sorensen et al. (1997) studied similar Franciscan rocks and concluded that K was added during the metasomatic processes that accompanied metamorphism of blueschist to eclogite. Na alteration (spilitization) of ocean-floor rocks is common, but K enrichment, which accompanies palagonitization, is usually confined within the topmost few hundred meters of ocean-floor rocks (Ridley et al., 1994). Inasmuch as the Franciscan blocks of our study possibly belonged to the topmost layer of the subducted crust, it would not have been uncommon for them to have had Na and K enrichment before subduction. The low SiO_2 exhibited by some of the garnet amphibolites and eclogites cannot be explained by alteration of N-MORB unless their protoliths formed in the mantle as low-SiO_2 arc tholeiites. The high SiO_2 content of a garnet amphibolite (sample Q1–2) reflects the significant amount of quartz in this sample, as observed petrographically, which may be related to the presence of metachert layers as seen by the presence of a microfolded Mn-garnet layer in this rock (see Appendix, Fig. A1). Overall, major element compositions, without considering the seafloor alteration effects, indicate that arc tholeiites are possible protoliths of the high-grade blocks, whereas for the protoliths to be N-MORBs, they would have had to require some metasomatic process of silica depletion and enrichment prior to subduction. Also, some "nugget effect," nonrepresentative of the coarse-grained bulk-rock samples (especially the banded rocks), might have altered the powders prepared for whole-rock major elemental analysis and led to the variation observed in the SiO_2 content seen in these rocks. Thus, major element considerations alone indicate that the high-grade rocks of this study may have both MORB-like as well as arc-tholeiite–like geochemical features, indicating that perhaps both types of rocks were protoliths of these high-grade blocks. There is little indication in the major element compositions of these rocks of the presence of ocean-island–type volcanic rocks as protoliths.

The overall REE patterns in Figure 2 are similar to arc basalts (Hawkesworth et al., 1977; Tatsumi and Eggins, 1995) and are distinctly different from OIB. The Western Pacific arc tholeiite REE data (Jakes and Gill, 1970) are shown by the shaded regions in Figure 2. Although the REE patterns, especially of the blueschists (Fig. 2) of these Franciscan rocks, are similar to those of some typical MORB, the blueschist, eclogite, and garnet amphibolite data also overlap the Western Pacific arc tholeiite REE data. The absence of conspicuous LREE-enriched patterns indicates that no continental component (including continent-derived sediments) was present in the high-grade blocks, which is also validated by the absence of high-grade metasediments in the Franciscan. Pb isotopic data, as discussed later, also support the hypothesis that no continental component is present in these rocks. If arc tholeiites or MORB were the precursors of these rocks, our data would imply that the transformation of these tholeiites to blueschists and eclogites was not accompanied by large-scale LREE mobilization during subduction; these elements were merely redistributed among the newly formed minerals, such as lawsonite, titanite, allanite, garnet, and omphacite (Tribuzio et al., 1996), without significant release of REE to the overlying mantle wedge. Thus from the REE data we can conclude that either MORB or arc tholeiites could be the protoliths of these high-grade blocks.

In Figure 3, with the exception of two low ε_{Nd} samples, most of the rocks in this plot could be characterized as either having seawater-altered MORB or arc tholeiite as protoliths. The low initial ε_{Nd} signatures were identified in previous studies (Nelson, 1991, 1995) and were interpreted as alteration by fluids derived from subducted continental sediments. However, this conclusion was based on Nd and Sr isotopes alone, whereas our interpretations are based on a more extensive data set that includes Pb isotopes, major elements, REE, and HFSE, in addition to Nd and Sr isotopic data. The two samples (Q1–2 and TIBB-2) contain a significant amount of quartz. The quartz-rich nature of these samples suggests that their protoliths may have contained nonbasaltic lithologies such as chert. Sample Q1–2 exhibits tightly folded layers of spessartine garnet that likely represent metamorphosed and folded chert layers or lenses within what would otherwise be metabasaltic rock. A photomicrograph (Appendix, Fig. A1) shows a microfolded layer of manganiferous garnets within this quartz-bearing garnet amphibolite. The garnet-rich layers in such rocks are generally regarded as relics of metachert layers within the protoliths of the garnet amphibolite. It should also be noted that the presence of such metachert layers would cause major element chemical heterogeneity in the protoliths by silica addition, as well as in the Nd and Sr isotopic compositions of the bulk rocks by inheriting seawater Nd and Sr in the chert layer. This effect is seen in two rock samples in the Nd-Sr isotope ratio plot of Figure 3 and in samples of garnet amphibolites like sample Q1–2. Isotopic and chemical compositions of bedded radiolarian cherts, as found in the Franciscan, are mostly dominated by biogenic silica derived from radiolarian and sponge spicules, and modified by the addition of authigenic hydrogenous components (Shimizu et al., 2001). Thus, radiolarian chert could account for the low ε_{Nd} values seen in these high-grade rocks. We also note here that the lack of published Nd and Sr data for samples of the Coast Range Ophiolite do not allow a much-needed comparison with the rocks of this study (J.W. Shervais, 2003, personal commun.).

In Figure 4, the high-grade blocks plot on the field of oceanic basalts near the NHRL, away from the EMII reservoir. Pb isotopes are sensitive indicators of local sediments in the subduction zone; typically many subduction zone magmas exhibit steep arrays on $^{206}Pb/^{204}Pb$ versus $^{207}Pb/^{204}Pb$ and $^{208}Pb/^{204}Pb$ plots (Hawkesworth et al., 1977; Meijer, 1976), implying sediment involvement in island-arc basalt genesis. It is most likely that in such instances, arc Pb is contributed by subducted sediments and from slab-derived fluids. As noted previously, the lack of conspicuous LREE-enriched patterns also suggests a lack of a continental crust component. These observations rule out continental crustal Pb in the protoliths of these HP-LT metamorphic rocks. Thus we infer that the Pb in the high-grade Franciscan rocks was almost entirely derived from a MORB-like depleted mantle source with little contribution from continental sources and sediments. The similarity between the Coast Range Ophiolite, which is believed to have arc crust (Giaramita et al., 1998), and the Franciscan samples in terms of Pb isotopic values, supports the contention that arc tholeiites are viable protoliths of the Franciscan samples.

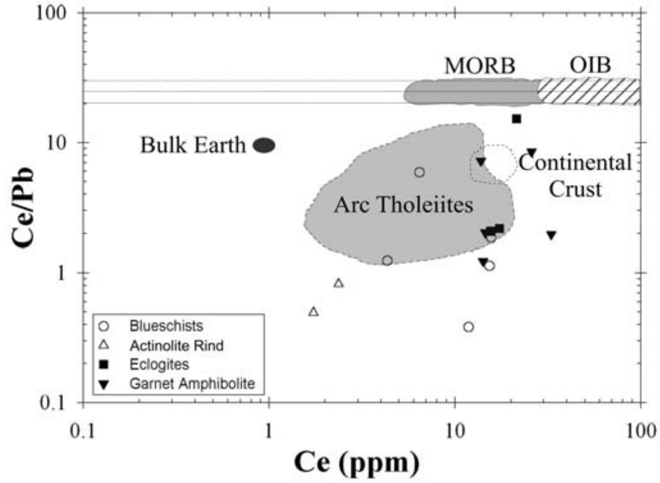

Figure 5. Ce/Pb ratios and Ce concentrations in Franciscan rock samples in comparison with fields for oceanic basalts (MORB and OIB), global arc lavas, average continental crust, and the chondritic bulk-earth composition. Note non-MORB– and non-OIB–like compositions of the Franciscan high-grade metamorphic rocks of this study, suggesting subducted arc basalts as protoliths of these Franciscan rocks. Some Pb mobilization also took place during Franciscan subduction, as discussed in the text. Other data sources are from Hofmann et al. (1986) and Miller et al. (1994).

Consideration of Ce/Pb ratios (Fig. 5) for the eclogites and blueschists can be useful regarding protolith origin, especially in light of the initial Pb isotopic ratios of the same rocks as previously discussed. Ce/Pb ratios are, in general, remarkably uniform in both MORB and OIB rock types (Hofmann et al., 1986), with a value of 25 ± 5. Continental crust, however, has a much lower value of 4. Considerable discussion in the literature concerns the preferential partitioning of Pb, apparently by a continuing geological process from the mantle into the continental crust via some nonmagmatic transfer of Pb during the subduction process (Miller et al., 1994). The strong correspondence of the Franciscan Ce/Pb ratios with arc lavas is clear, although this similarity may also be due to the mobility of Pb during subduction. However, the foregoing discussions of the major element, REE, Sr, Nd, and Pb isotopic ratios are consistent with an arc tholeiitic parentage for the high-grade blocks. Our preference for an arc origin of the high-grade block protoliths is also supported by the N-MORB–normalized multiple element considerations as discussed later.

The rocks show low Nb/U values, the Nb/La values vary between 0.3 and 1.3, and the MORB value is 0.9. The high concentration of Nb is due to the presence of rutile (see Appendix), as indicated by the TiO_2 concentrations. Because arcs are not depleted in La in comparison to Nb, the low Nb/La ratios also indicate that the protoliths of these rocks were Nb depleted. Again, higher Nb/La values in a few samples (Table 1) could be attributed to the presence of titanite and rutile. The low Ce/Pb and Nb/U ratios in most of the samples are significant because of the documented mobility of Pb and U during subduction processes. The question arises, then, as to whether this mobilization took place during Franciscan subduction or was already recorded in the arc protoliths of the high-grade Franciscan blocks.

Multiple trace element concentrations (Table 1) are important for resolving the issue

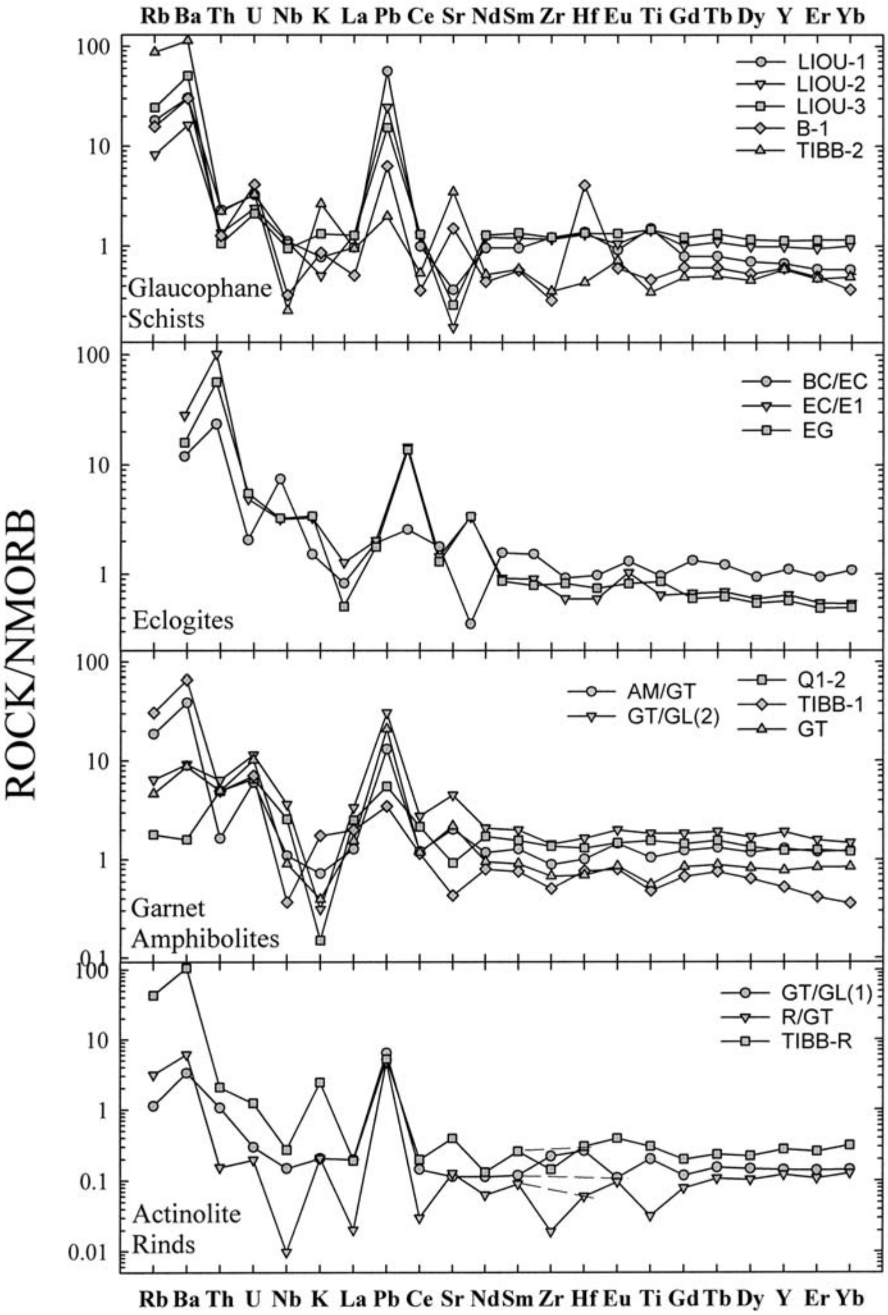

Figure 6. Multiple trace element concentrations normalized to N-MORB for the high-grade Franciscan metamorphic rocks. Elements are arranged according to progressively varying incompatibility (Tatsumi and Eggins, 1995). Along with low Ce/Pb, Nb/U, the generally high Ba/Rb and Ba/Th enrichments and the inordinately high Pb enrichments of these rocks are noteworthy. The overall trace element signatures of these rocks are clearly unlike MORB but similar to arc basalts, with some enrichment of fluid-mobile elements like Pb, Ba, Rb, and U, during Franciscan subduction.

of protoliths—whether they were MORB or arc tholeiites. N-MORB–normalized multiple trace element patterns are shown in Figure 6. These normalized trace element patterns can be diagnostic of subduction zone fluids as well as those of arc volcanic rocks. Arc rocks are believed to acquire this trace element signature by partial melting when fluids, formed by the dehydration and devolatilization of the subducting oceanic slabs, react with the depleted mantle wedge, causing this melting and ultimately forming lavas with characteristic arc signatures. Nb depletion is clearly seen in the blueschists and garnet amphibolites in their trace element patterns. The high Ba/Nb, U/Th, and Pb/La ratios in these Franciscan rocks are significant (Fig. 6). Ba and Pb have concentrations that reach up to 100 times or more the average upper crust composite (Hart and Staudigel, 1989) and more than 2 times Ba and 5 times Pb of the most enriched subduction zone basalts (Tatsumi and Eggins, 1995). N-MORB–normalized values of Th, an immobile element, in general are greater than 1 in the high-grade rocks. Thus, the rocks of our study could not be so enriched in Th, along with Ba and Pb (Fig. 6), by fluids from the subducting slab unless the rocks themselves underwent an episode of melting during Franciscan subduction, which is unlikely. Thus, arc basalts, which would have formed from partial melting of the mantle wedge, would have to constitute the protoliths of the Franciscan rocks to retain this enriched Th, Ba, and Pb signature. Thus, we believe that arc tholeiites would be a stronger candidate for the protoliths of the high-grade blocks.

Actinolite Rinds

Geochemical Data

Chondrite-normalized REE patterns for the actinolite rinds, displayed in the lowest panel of Figure 2, show low concentrations and flat to LREE-depleted patterns. La concentrations vary between 0.2 and 2 times chondrite. These actinolite rinds show a wide range of ratios—0.1–1.1 for $(La/Sm)_n$ and 0.7–1.1 for $(Gd/Lu)_n$. They plot below the field of the Pacific arc tholeiites (Fig. 2) and are unlike the REE patterns of the high-grade blocks. In Figure 3, the three actinolite rinds plot away from the region of arc tholeiites with low initial ε_{Nd} (+1.2 to +4.0) and high initial $^{87}Sr/^{86}Sr$ (0.70516 to 0.70849). In the Pb isotopic plots the actinolite rinds fall in the same region as the high-grade blocks, close to the NHRL and in the field of the oceanic basalts. Hence, they are not shown by separate symbols. In the Ce/Pb versus Ce plot of Figure 5, two of these samples plot below the field of the arc tholeiites; sample R/GT was not plotted because of its very low Ce concentration (0.4 ppm). In N-MORB–normalized compatible and incompatible trace element plots (lower panel, Fig. 6) they show LILE and Pb-K enrichment, similar to the high-grade blocks.

Discussion

In the major element compositions, the actinolite rinds are chemically distinctly different from the rocks of the high-grade blocks. They are MgO enriched and low in Al_2O_3 in comparison to the rest of the rocks of this study. This observation clearly indicates that they are different from the high-grade blocks. The rinds are possibly the most metasomatized parts of the high-grade blocks. The chondrite-normalized REE patterns of the rinds indicate that the concentrations of trace elements are low in comparison to the high-grade blocks. These REE patterns also indicate, as in the case of the high-grade blocks, that no crustal component was involved during the metasomatism of these rinds. The low initial ε_{Nd} and the high initial $^{87}Sr/^{86}Sr$ ratios, and the lower Nd and Sr contents (Table 2; Fig. 3) of the actinolite rinds, could be due to seawater alteration and/or continental crustal contamination of the protoliths of the actinolite rinds (Fig. 3). The Pb isotopic ratios (Fig. 4A, B) rule out the possibility of crustal contamination. Thus, a component with crustal Nd and Sr, but no crustal Pb, is needed as the source for the three rocks with low ε_{Nd} values. Phosphate from fish debris that scavenges REE from seawater with low ε_{Nd} and radiogenic, seawater-derived Sr (Elderfield and Pagett, 1986) could explain these anomalous isotopic compositions. Alternatively, biogenic silica from bedded radiolarian chert (Shimizu et al., 2001), as mentioned previously in the case of high-grade blocks, could also be a possible candidate. Thus, these three samples (with open symbols) in the lower right of Figure 3 may contain the fish-debris phosphate or chert component in their protoliths. However, Pb isotopic ratios indicate an absence of crustal components in these rinds, as also validated by the REE patterns. The samples under discussion have Ce concentrations from 0.4 to 2.4 ppm, whereas Ce/Pb ratios vary at ~1 or below (Fig. 5). They plot away from the high-grade blocks, indicating more Pb enrichment in comparison to the high-grade blocks during metasomatism. The actinolite rinds show K enrichment coupled with LILE and Pb enrichment (Fig. 6). Thus, the combined major element, trace element, and isotopic data of the actinolite rinds seem best explained by the metasomatism of a depleted mantle-wedge ultramafic rock by typical subduction zone fluids. However, we note here that the high-grade blocks may also have interacted with this fluid, but they show less of an effect in their trace element and isotopic signatures because of initially higher trace element contents in their protoliths.

Conclusions from Geochemical Data

The major element chemical variation seen in the high-grade blocks might be considered to be the near original composition of most of these rocks because of their isotopic and trace element signatures. The lack of strong LREE enrichment, for example, in the high-grade blocks indicates that element mobility in these high-grade blocks has been minimal. Thus, the geochemical results discussed previously can be generally interpreted to indicate an island-arc-basalt protolith for the Franciscan high-grade blocks from Ring Mountain (Fig. 1A, B). The major element compositions indicate that the high-grade blocks could possibly be either MORB or arc tholeiites. REE patterns of the samples in this study are similar to both N-MORB and arc tholeiites. The Nd and Sr isotopic data fall near the fields of arc tholeiites, with the exception of a few samples that might contain some oceanic crustal component from seawater-derived Nd and Sr additions. Both the REE patterns and the Pb isotopic ratios indicate the absence of continental crustal components in their protoliths. Ce/Pb and Nb/U ratios suggest that Pb and U could have been mobile to some extent during Franciscan subduction. The Nb depletion generally seen in these rocks cannot be a feature acquired during Franciscan subduction. Concentrations of Th, an immobile element, are found to be higher in the studied samples than N-MORB, indicating that these characteristics were inherited in an arc tholeiite protolith because these high-grade blocks did not suffer partial melting during subduction, which would have caused enrichment in Th. The fact that all these geochemical signatures have been faithfully retained in the Franciscan eclogites and blueschists, despite their HP-LT metamorphism in the subducted slab some 160 m.y. ago, attests to the validity of our geochemical approach in testing whether the arc basalts were the protoliths of these rocks. Collectively, all the geochemical data presented here implicate predominantly arc basalts as protoliths of the high-grade blocks, with additional imprints perhaps having acquired major element, trace element, and isotopic characteristics during Franciscan subduction within the slab-by-slab–derived fluids. Samples of actinolite rinds were too metasomatized to be used in defining the protoliths of those rocks.

It is clear from this discussion that the geochemical signatures of some of the samples may be similar to MORB, although it is not uncommon for arc regions to contain N-MORB–like rocks in terms of their geochemical and isotopic characteristics (Caprarelli and Leitch, 2002; DeBari et al., 1999; Johnson and Fryer, 1990). It is noteworthy that the Coast Range Ophiolite contains a diversity of basalts, including island-arc tholeiites as well as supra-subduction-zone–related MORB components (Giaramita et al., 1998; Shervais, 2001). Therefore, even though some samples of the Franciscan of this study may show N-MORB–like characteristics, they do not require the protoliths of all the high-grade rocks of this study to have formed in a MORB-like setting.

TECTONIC EVOLUTION OF FRANCISCAN HIGH-GRADE BLOCKS

Geochemical data from Franciscan high-grade blocks from Ring Mountain indicate an infant-arc origin for these rocks, similar to that proposed for the Coast Range Ophiolite, and are different from the origin of other Franciscan metavolcanic rocks studied thus far. Some previous studies have dealt with incipient blueschist facies or lower-grade Franciscan volcanic rocks with preserved relic igneous mineralogy and textures (MacPherson et al., 1990), but they are not relevant to problems related to higher-temperature metamorphism associated with the inception of subduction that is recorded in high-grade blocks. The trace element study of Ward Creek metabasites, among the oldest and highest-grade coherent metabasites, suggested an oceanic arc protolith for those rocks similar to our conclusions for the high-grade blocks (Swanson et al., 2004). In studies of high-grade blocks of the Franciscan (Nelson, 1991, 1995; Sorensen et al., 1997), protoliths were considered to be of MORB origin, with fluids that modified the block composition having originated from high-grade metasediments, based on trace elements or Sr/Nd isotopic ratios. But our combined study of trace and major elements, along with Nd, Sr, and Pb isotopic ratios, indicates that some of the protoliths of the high-grade blocks had an arc origin and that none of the blocks appears to possess a chemical component derived from a continental source, such as high-grade metasedimentary rocks.

On the basis of the geochemical evidence presented previously, a model for the development of the high-grade blocks and the Coast Range Ophiolite is now described (Fig. 7), which is modified from Wakabayashi and Dilek (2003).

Initiation of west-dipping subduction occurred as a result of a collision somewhere along the boundaries of the plates involved (Mueller and Phillips, 1991). Initiation of subduction caused displacement of the underlying asthenosphere, which, being lighter, migrated upward, causing stretching of the younger lithospheric plate, followed by seafloor spreading (Fig. 7A). Adiabatic decompression of the upward moving asthenosphere, combined with the dehydration of the subsiding lithosphere, would have caused widespread melting. This melting would have led to the formation of infant-arc crust by seafloor spreading; melts that characterize this geologic situation would be of boninitic affinities. As a consequence of the rapid subsidence of the downgoing plate, the

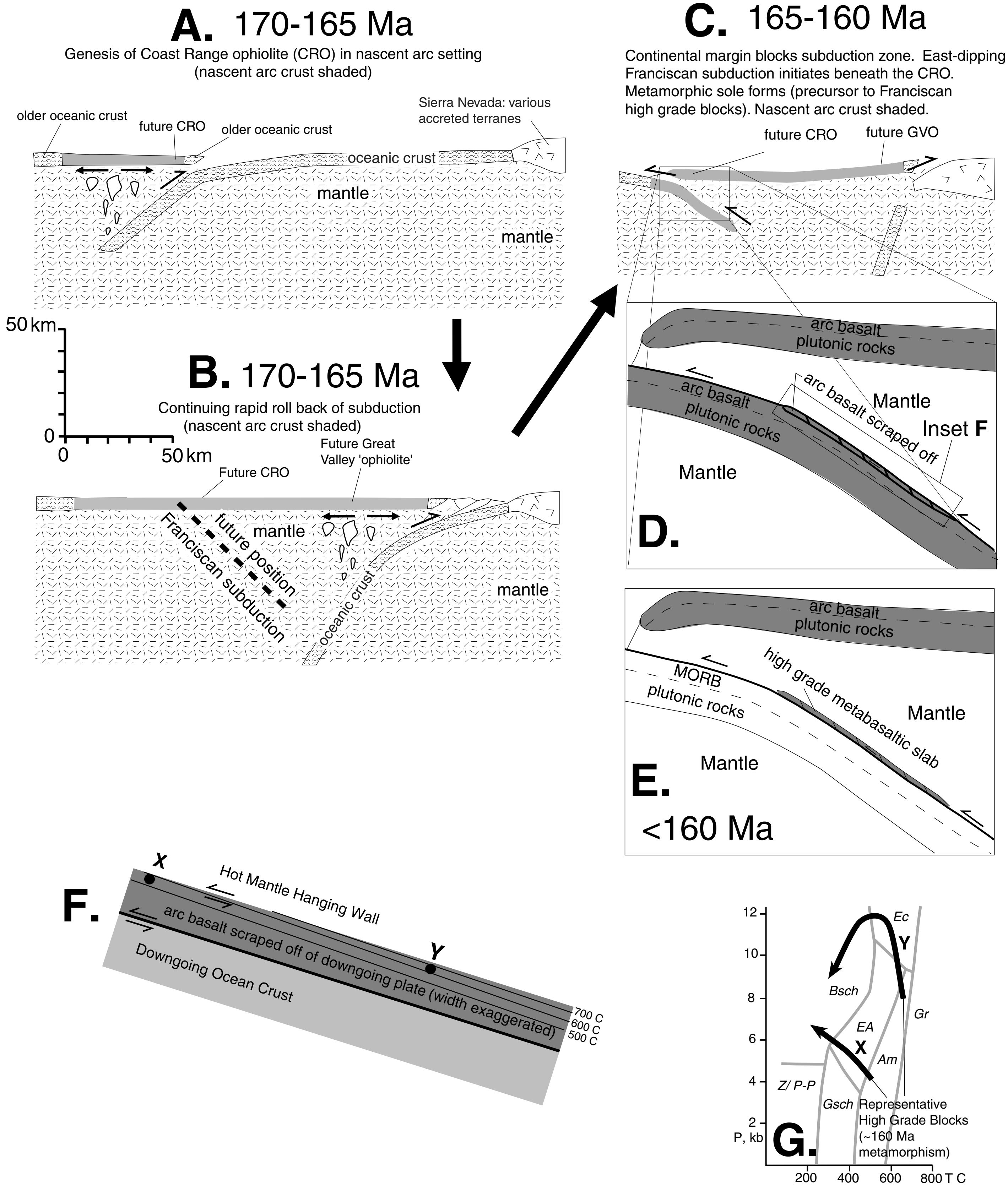
A. 170-165 Ma
Genesis of Coast Range ophiolite (CRO) in nascent arc setting
(nascent arc crust shaded)
older oceanic crust
future CRO
older oceanic crust
Sierra Nevada: various accreted terranes
oceanic crust
mantle
mantle
50 km
0
0
50 km
B. 170-165 Ma
Continuing rapid roll back of subduction
(nascent arc crust shaded)
Future CRO
Future Great Valley 'ophiolite'
mantle
future position
Franciscan subduction
oceanic crust
mantle
C. 165-160 Ma
Continental margin blocks subduction zone. East-dipping Franciscan subduction initiates beneath the CRO. Metamorphic sole forms (precursor to Franciscan high grade blocks). Nascent arc crust shaded.
future CRO
future GVO
arc basalt
plutonic rocks
arc basalt
plutonic rocks
arc basalt scraped off
Mantle
Inset F
Mantle
D.
arc basalt
plutonic rocks
MORB
plutonic rocks
high grade metabasaltic slab
Mantle
Mantle
E.
<160 Ma
F.
X
Hot Mantle Hanging Wall
arc basalt scraped off of downgoing plate (width exaggerated)
Y
Downgoing Ocean Crust
700 C
600 C
500 C
12
10
8
6
4
2
P, kb
Ec
Y
Bsch
Gr
EA
X
Am
Z/ P-P
Gsch
Representative High Grade Blocks (~160 Ma metamorphism)
G.
200
400
600
800 T C

subducting slab rolled back, and this rollback was paired with the extension of the lithosphere above it, creating arc crust (Fig. 7B). Rocks with boninitic affinities are found in the Josephine ophiolite (Crawford et al., 1989) and the Coast Range Ophiolite (Shervais, 2001), indicating that an arc environment was present at the western margin of North America. The Coast Range Ophiolite and protoliths of the Franciscan high-grade blocks are suggested to have formed in this infant-arc environment.

Although the Coast Range Ophiolite was formed in an infant arc environment associated with young subduction, it was not emplaced over the subduction zone it formed (Wakabayashi and Dilek, 2000). This is because the age of high-temperature metamorphism of the high-grade blocks that marks the initiation of Franciscan subduction is younger than the age of the Coast Range Ophiolite. For this ophiolite to have been formed above the east-dipping Franciscan subduction zone, the age of high-grade metamorphism in the high-grade blocks would have had to be older than the ophiolite (see Wakabayashi and Dilek, 2000, and references therein). No metamorphic rocks found structurally beneath the Coast Range Ophiolite are older than the ophiolite. If an older, east-dipping subduction zone existed, *all* evidence for it must have been removed by strike-slip faulting or other processes. Consequently, it is more likely that a pre-Franciscan, west-dipping subduction zone was related to the formation of the Coast Range Ophiolite (Fig. 7A, B), as proposed by several workers (Dickinson et al., 1996; Moores, 1970; Schweickert and Cowan, 1975). In contrast to the lack of evidence for pre–Coast Range Ophiolite subduction within or west of the Franciscan Complex, there is abundant evidence of pre-Franciscan subduction in the Sierra Nevada, although the polarity of the various episodes of subduction recorded in the Sierra Nevada basement are not agreed upon by all workers (e.g., Dickinson et al., 1996; Moores, 1970; Saleeby, 1992). Gravity, magnetic, and seismic data indicate the presence of a buried west-dipping zone of mantle material (10 km or more thick) beneath the Great Valley, and this structure has been interpreted as a west-dipping suture zone (Godfrey and Klemperer, 1998; Godfrey and Dilek, 2000). It is not certain as to whether this apparent suture "daylights" in the western Sierra Nevada (Godfrey and Dilek, 2000). Wakabayashi and Dilek (2000) proposed that garnet amphibolites beneath the Jarbo Gap ophiolite and garnet amphibolite, associated with the Tuolumne Complex in the western Sierra Nevada (the latter yielding a 178 Ma Ar/Ar age; Sharp and Leighton, 1987), may have been formed during the inception of a west-dipping subduction zone; this paleosubduction zone may be associated with the buried mantle suture, or it may represent a separate suture.

The infant arc origin of the Franciscan high-grade block protoliths, as determined in this study, also indicates that a pre-Franciscan subduction zone must have been associated with the generation of the high-grade-block protoliths. The igneous protoliths could not have been formed in the same (Franciscan) subduction zone that metamorphosed them, given that the metamorphism that they underwent could have occurred only at the inception of subduction.

Our proposed model for the initiation of Franciscan subduction and the origin of the Coast Range Ophiolite in an infant arc setting, although similar in many ways, differs from that proposed by Stern and Bloomer (1992) in one significant aspect—that of the polarity of initial subduction. These authors suggested that the Coast Range Ophiolite formed over an east-dipping Franciscan subduction zone. The formation of the ophiolite over the Franciscan subduction zone is inconsistent with the fact that high-grade blocks are younger than the ophiolite. Although it may be argued that some high-grade-block ages are so close to those of the Coast Range Ophiolite that it is difficult to determine which is older (counter-arguments to this are presented in Wakabayashi and Dilek, 2000), the fact that the protoliths of the high-grade blocks are themselves of infant arc origin argues for the presence of a pre-Franciscan subduction zone. As discussed, the pre-Franciscan subduction zone is more likely west dipping than east dipping (Fig. 7A, B). U-Pb zircon ages of 178 ± 7.2 and 218.9 ± 6.0 Ma were obtained from euhedral and anhedral zircon grains, respectively, from a Franciscan high-grade block (Page et al., 2003). This might be taken as evidence of older Franciscan subduction that predated the Coastal Range Ophiolite and evidence supporting formation of the ophiolite over an east-dipping Franciscan subduction zone. However, consideration of the 178 Ma age as a high-T metamorphic age of the block demands an unlikely scenario of metamorphic temperatures remaining above Ar closure in hornblende (~500 °C) for 15–18 m.y. after peak metamorphism. Following the initiation of subduction, refrigeration of the subduction zone occurred rapidly, and it is not likely that it would take 15–18 m.y. for the high-grade blocks to cool from peak metamorphic temperatures to 500 °C, (e.g., Hacker, 1991). Another alternative scenario for

Figure 7. This series of diagrams summarizes the general tectonic development of the high-grade blocks, similar to those found at Ring Mountain. (A, B) West-dipping subduction begins, and the slab rapidly rolls back eastward, with lithospheric extension above and the formation of nascent arc crust, including that of the Coast Range Ophiolite and the protoliths of the high-grade blocks such as at Ring Mountain. (C) East-dipping Franciscan subduction initiates as a result of the blockage of the west-dipping subduction zone. The new subduction zone initiates within the infant-arc crust. (D, E) Enlargements of the young Franciscan subduction zone, showing the offscraping of nascent arc basalt to form the high-grade blocks and later subduction of oceanic crust of MORB and OIB affinity. The initial subduction of the high-grade blocks results in high-temperature metamorphism, which varies in temperature and pressure as a function of how close the rock is to the hanging wall of the subduction zone and how far it is down the dip of the subduction zone when it is offscraped (F). This results in a variety of pressure-temperature (*P-T*) conditions for high-grade metamorphism found in the blocks. As subduction continues, the offscraped basaltic material quickly cools and a counterclockwise *P-T* path results (G). The pressure increase (vertical scale) shown in (G) may result from thrust imbrication of the upper plate, or partial resubduction of the blocks after peak (temperature) metamorphism. Note that the width of the slab of basalt, the subject of high-grade metamorphism, is greatly exaggerated in (D), (E), and (F) so that it is visible. Following the underplating of the metamorphic rocks, the metamorphic sheet was dismembered, so that most of this material is found now only as blocks in shear zones. In (G): Z/P-P—zeolite–pumpellyite-prehnite facies; Bsch—blueschist facies; Ec—eclogite facies; Gr—granulite facies; EA—epidote-albite facies; Am—amphibolite facies; Gsch—greenschist facies. Note initially high temperature of metamorphism (horizontal scale), as would be expected in the subducted nascent arc crust as proposed in this study. Subsequent cooling during subduction results in the counterclockwise *P-T* path as shown in this diagram, which is based on previous studies. Diagrams based in part on Wakabayashi (1999).

high-grade-block evolution might be cooling after initiation of subduction, followed by reheating in a ridge-subduction event, but such a scenario is not likely based on the prograde *P-T* paths that show evidence for subduction rather than two distinct stages of high-T metamorphism (e.g., Krogh et al., 1994). Shervais (2001) proposed that high-grade block metamorphism is a product of ridge subduction alone without an earlier metamorphic history. Such a scenario conflicts with the fact that the high-grade blocks or any adjacent units lack low-P–high-T metamorphism (high-grade–high-T block metamorphism is medium to high pressure) that should be expected from ridge-subduction metamorphism (Brown, 1998; Sisson and Pavlis, 1993). It is likely that the older zircon ages from the high-grade blocks are a product of igneous or metamorphic zircon crystallization related to pre-Franciscan west-dipping subduction rather than to pre–Coast Range Ophiolite Franciscan subduction.

Our model for the origin of the Franciscan high-grade blocks on the basis of our geochemical data is consistent with models that suggest metamorphism occurred at the inception of subduction beneath the young Coast Range Ophiolite (Hanan et al., 1992; Wakabayashi, 1990; Wakabayashi and Dilek, 2000). Arc geochemistry suggests that east-dipping Franciscan subduction was initiated within the young infant arc crust (Fig. 7B, C, D) as a consequence of the blockage of the earlier west-dipping subduction zone by the continental margin. Continued subduction resulted in the offscraping of rocks of MORB or OIB origin from farther west, away from the subduction zone (Fig. 7E, F).

The *P-T* path that developed in the high-grade blocks depended in part on the original position of high-T metamorphism (Wakabayashi, 1992, 1999) as shown schematically in Figure 7G for *P-T* paths labeled X and Y in Figure 7F. The pressure increase noted during cooling may be related to imbrication or thickening of the upper plate or partial resubduction of pieces from the high-grade slab. Continued shearing of the metamorphic slab resulted in disruption of the slab into blocks in a shear zone. These are the high-grade blocks of the Franciscan in our model.

Based on $\delta^{18}O$ variability within the minerals (Taylor and Coleman, 1968) of the subducted Franciscan high-grade rocks, such as eclogites and glaucophane schists, it appears that these rocks could not have formed by oxygen-isotopic exchange solely with typical mantle reservoirs. Rather, these rocks were imprinted by the oxygen isotopic signatures of crustal fluids (Magaritz and Taylor, 1976); preliminary results as presented here indicate that this fluid source was hydrothermally altered submarine igneous rocks in an island-arc environment.

CONCLUSIONS

High-grade-metamorphic rocks from Ring Mountain of the Franciscan Complex have arc basalts as protoliths. Multiple trace element and isotopic geochemical characteristics of the Franciscan blueschists and eclogites provide evidence that the protoliths of these rocks were arc basalts. The geochemical characteristics of the high-grade blocks described here suggest a common origin with the Coastal Range Ophiolite and indicate that Franciscan subduction initiated within infant-arc crust that formed over a pre-Franciscan subduction zone. With further subduction, older oceanic crust of MORB and OIB affinity was subducted, with some pieces being offscraped to form most of the lower grade volcanic rocks within the Franciscan Complex during thermal relaxation. Some low-grade volcanic and plutonic blocks in Franciscan mélanges are of arc origin and appear to have been derived from parts of the Coast Range Ophiolite that were exhumed and eroded comparatively early in the history of Franciscan subduction and shed as olistostrome blocks into the Franciscan trench (MacPherson et al., 1990; Erickson et al., 2004).

To be certain that the results from Ring Mountain are applicable to all Franciscan high-grade blocks, further studies of other localities in the Franciscan are desirable. Possibly one may discover substantial heterogeneity and multiplicity of the petrotectonic sources of the blocks. The trace element study of the Ward Creek metabasites (Swanson et al., 2004) suggests an arc protolith for those rocks and suggests that arc crust may have been subducted for the first 20 m.y. of Franciscan subduction. Further studies of coherent blueschists of different metamorphic-accretionary ages may facilitate estimates of the duration of subduction of arc crust and estimates of the width of the original arc-generated crust.

APPENDIX

Sample Localities and Petrographic Descriptions

The following are brief petrographic descriptions of the various high-grade-block samples and the localities (see Fig. 1B) from which they were collected.

LIOU 1, 2, and 3 are all blueschist samples from the same block on the south side of Ring Mountain. They are fairly similar except that LIOU 2 lacks garnet and has albite.

LIOU 1: The mineral assemblage is sodic amphibole + white mica + lawsonite + garnet + titanite + hematite. There is some early clinozoisite-epidote and late chlorite. The garnet may be a relic from an earlier stage of crystallization.

LIOU 2: The mineral assemblage is sodic amphibole + white mica + epidote-clinozoisite + albite + titanite + hematite. Lawsonite is present as in LIOU 1 and is clearly texturally late, exhibiting a poikiloblastic texture.

LIOU 3: The mineral assemblage is sodic amphibole + white mica + lawsonite + garnet + titanite + hematite. There is some early clinozoisite-epidote and late chlorite.

AM/GT, GT, GT/GL 1, B 1, and R/GT are all taken from the same garnet amphibolite block on the north side of Ring Mountain; these samples represent different parts of the block, including a sample with nearly complete blueschist recrystallization and the rind.

AM/GT: This is a garnet amphibolite with a small amount of blueschist retrograde metamorphism manifested in sodic amphibole rims on calcic amphibole. The high-temperature assemblage is calcic amphibole + garnet + epidote-clinozoisite + white mica + rutile + hematite ± albite (texturally late in this sample). Titanite rims rutile and locally forms poikiloblastic grains. Sodic amphibole rims the calcic amphibole, and late chlorite occurs locally. The calcic amphibole composition is probably similar to that of TIBB (discussed later) on the basis of its appearance.

GT: This is a garnet amphibolite with a small amount of blueschist overprinting, as just described. This sample differs from AM/GT in that it lacks albite. The high-temperature assemblage is calcic amphibole + garnet + epidote-clinozoisite + white mica + rutile + hematite. Titanite rims rutile, and sodic amphibole locally rims calcic amphibole. Late chlorite also occurs in this sample. Small zircons are present and are most noticeable as small inclusions in the calcic amphibole.

B 1: This is a blueschist sample that comes from one of the outer layers of the garnet amphibolite block. Because of this relationship, one would infer that it was originally garnet amphibolite, although none of the high-temperature assemblage remains in this sample. The mineral assemblage is sodic amphibole + epidote-clinozoisite + white mica + hematite. Late poikiloblastic lawsonite is common in this sample. Titanite may occur as fine grains in this sample, but if so, it is not common.

GT/GL 1: This sample at first glance appears like an actinolite rind sample from this garnet amphibolite block. Alternatively this sample may be from one of the calcic amphibole-rich zones that appear to be dikes that cut across the block. The mineral assemblage is calcic amphibole + white mica + rutile. Sodic amphibole locally rims the calcic amphibole, and local rims of titanite occur on rutile grains.

R/GT: This is an unequivocal actinolite rind sample from this block. This sample is composed almost entirely of actinolite with some iron oxide and a little sodic amphibole rimming some of the actinolite. Titanite or rutile, if present, is not petrographically obvious.

EC and E-1 are from an epidote-rich eclogite block located near the garnet amphibolite block mentioned previously. Both of these samples exhibit little evidence of blueschist overprint.

EC: The mineral assemblage is omphacitic clinopyroxene + epidote-clinozoisite + garnet + rutile + hematite. Late chlorite occurs, and titanite has largely replaced rutile, leaving only local cores.

E-1: This sample is similar to EC.

Q1–2 and GT/GL 2 are taken from a quartz-bearing garnet amphibolite near the eclogite block noted above. Both garnet amphibole samples have minor amounts of blueschist facies overprinting in the form of sodic amphibole rims on calcic amphibole. Q1–2 differs significantly from GT/GL 2 in that clinopyroxene is present.

Q1–2: This is a quartz-bearing garnet amphibolite (Fig. A1). The high-temperature assemblage is

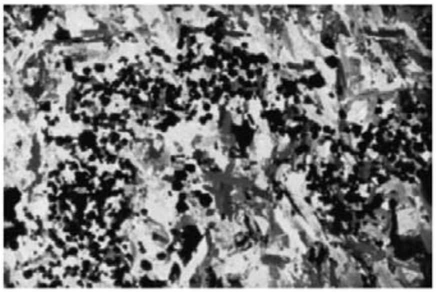

Figure A1. Photomicrograph showing a microfolded layer of manganiferous garnets within this quartz-bearing garnet amphibolite. It was taken under crossed nicols, and the length is 6 mm.

calcic amphibole + garnet + clinopyroxene + epidote-clinozoisite + quartz ± albite + iron oxides. Sodic amphibole locally rims calcic amphibole. Much of the clinopyroxene has been replaced by a fibrous yellowish to brownish red phase. Rutile or titanite is scarce or absent in this sample. The possibility of albite occurring with quartz, clinopyroxene, and garnet offers a rare opportunity to get a pressure estimate (from albite = jadeite + quartz) as well as a temperature estimate for this rock.

GT/GL 2: This is a quartz-bearing garnet amphibolite with a minor amount of blueschist overprinting. The high-temperature assemblage is calcic amphibole + garnet + epidote-clinozoisite + white mica + quartz + albite + rutile. Titanite has replaced most of the rutile, leaving just a few cores. Sodic amphibole locally rims calcic amphibole. Iron oxides either are absent or scarce in this sample.

BC/EC is taken from an eclogite block far down the northern slope of Ring Mountain above Marin County Day School. The block has a green and blue banded appearance from sodic amphibole-rich versus omphacite-rich layers. The eclogitic assemblage is omphacitic clinopyroxene + garnet + white mica + epidote-clinozoisite + rutile + iron oxides. Titanite has largely replaced rutile. Sodic amphibole is common in this rock; it appears to have largely formed after the eclogite assemblage. Some late chlorite is also present.

TIBB, TIBB 2, and TIBB R are taken from the same garnet amphibolite block on the south side of Ring Mountain. This is the same block that was sampled and labeled "TIBB" in Wakabayashi (1990).

TIBB: This sample is garnet amphibolite with minor blueschist overprinting. The high-temperature assemblage is calcic amphibole + garnet + epidote-clinozoisite + white mica + clinopyroxene + rutile + hematite. Most of the rutile has been replaced by titanite. Sodic amphibole locally rims calcic amphibole, and chlorite is also present. For more details on this rock, see Wakabayashi (1990). Small zircons are present and are most apparent as inclusions in the calcic amphibole.

TIBB 2: In this sample, blueschist assemblages have completely replaced earlier amphibolite assemblages. The assemblage present is sodic amphibole + white mica + epidote-clinozoisite + chlorite (mostly replacing what appears to have been garnet) + quartz + carbonate + titanite + hematite.

TIBB R: This is the actinolite rind from this block. The assemblage is actinolite + white mica + titanite, with some rimming of actinolite by sodic amphibole.

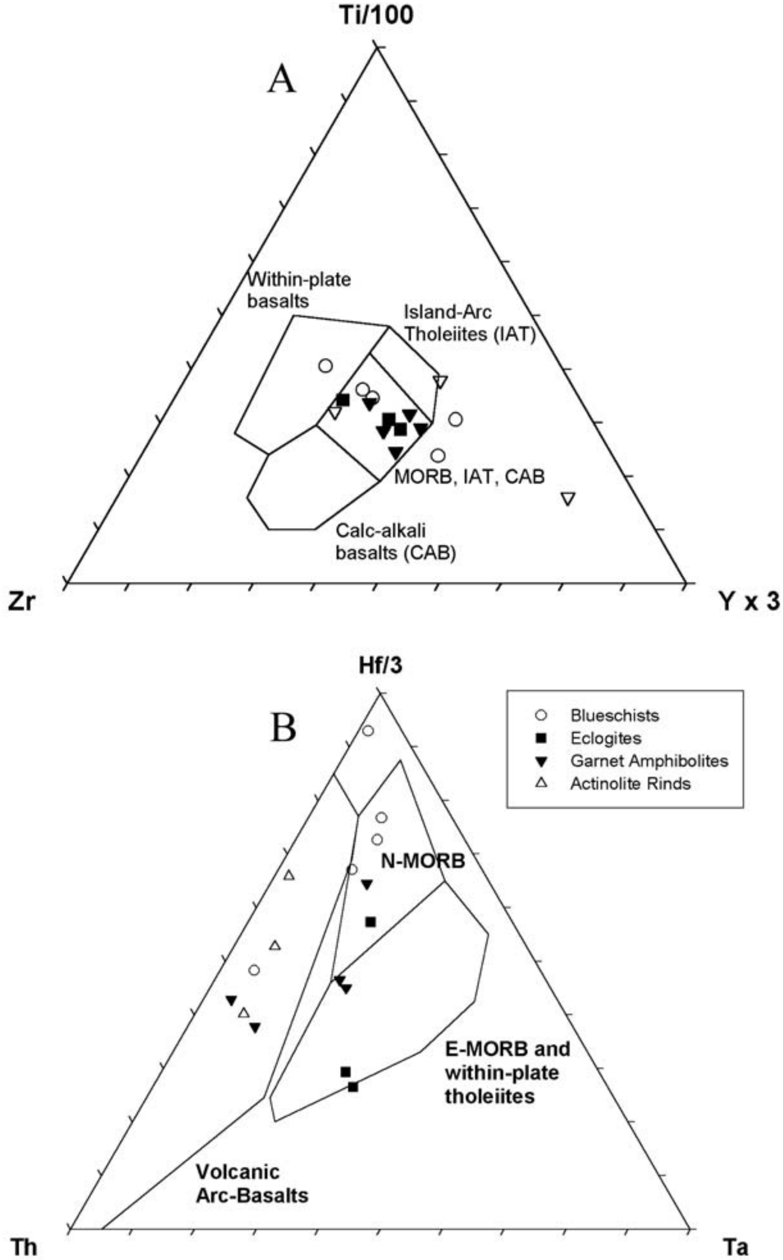

Figure A2. Tectonic discrimination diagrams using Ti, Zr, Y (A) and Hf, Th, Ta (B). Figure A2A shows the protoliths mostly in the MORB and are fields, whereas Figure A2B shows some of the garnet amphibolites and blueschists in the arc field, and most of the other rock samples falling in the margin between N-MORB and arc fields.

Additional Trace Element and Major Element Considerations

We provide some other tectonic discrimination diagrams for our data (Fig. A2A, B). These are Ti-Zr-Y and Hf-Th-Ta variation diagrams with different tectonic settings as distinguished by their respective fields. Notice that Figure A2A allows the protoliths to be both MORB and arc related, whereas Figure A2B indicates some amphibolites and blueschists to be arc basalts and most other rocks to plot marginally to the arc field. We also note that the Ta analyses by our ICP-MS method have larger errors.

In Figure A3, we plot the TiO_2 contents of the whole rocks against their FeO*/MgO ratios (all Fe as FeO*). Most of the amphibolites, blueschists, and eclogites show a narrow range in FeO*/MgO ratios, ranging from 1.5 to 2.5, whereas the TiO_2 content ranges from ~0.7 to 2.8 wt%. This variation could best be described by smaller variations in the modal mineralogy, such as in Fe-Ti oxides and titanite contents.

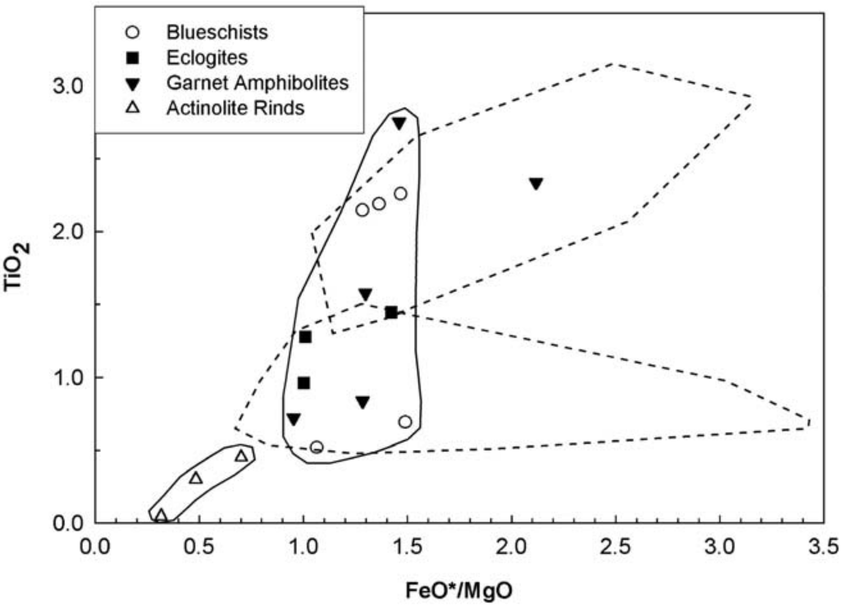

Figure A3. Variations in Tio$_2$ versus FeO*/MgO where FeO* is total Pe. Note narrow range in FeO*/MgO in most of the samples and larger variation in TiO$_2$ contents.

ACKNOWLEDGMENTS

We are grateful to S.B. Jacobsen and R.J. Stern for discussions regarding the geochemical interpretations of our data. We are also grateful to the Radiation Center, Oregon State University, Corvallis, for providing analysis of Hf and Nb. We thank J.W. Shervais for providing a preprint of one of his papers. We would like to thank R.J. Stern and J. Gill for reviewing an early version of this paper. This manuscript was considerably improved by the suggestions and criticisms of G. Ernst, J.W. Shervais, and associate editor P.R. Renne. This research was partially supported by U.S. National Science Foundation grants to A.R.B.

REFERENCES CITED

Anczkiewicz, R., Platt, J.P., Thirlwall, M.F., and Wakabayashi, J., 2004, Franciscan subduction off to a slow start: Evidence from high-precision Lu-Hf garnet ages on high-grade blocks: Earth and Planetary Science Letters, v. 225, p. 147–161, doi: 10.1016/j.epsl.2004.06.003.

Basu, A.R., Sharma, M., and DeCelles, P.G., 1990, Nd, Sr-isotopic provenance and trace element geochemistry of Amazonian foreland basin fluvial sands, Bolivia and Peru; implications for ensialic Andean Orogeny: Earth and Planetary Science Letters, v. 100, p. 1–17.

Blake, M.C., Jayko, A.S., McLaughlin, R.J., and Underwood, M.B., 1988, Metamorphic and tectonic evolution of the Franciscan Complex, northern California, *in* Ernst, W.G., ed., Metamorphism and crustal evolution of the western United States: Rubey Volume: Englewood Cliffs, New Jersey, Prentice Hall, p. 1035–1060.

Briqueu, L., Bougault, H., and Joron, J.L., 1984, Quantification of Nb, Ta, Ti and V anomalies in magmas associated with subduction zones: Petrogenetic implications: Earth and Planetary Science Letters, v. 68, p. 297–308.

Brown, M., 1998, Ridge-trench interactions and high-T–low-P metamorphism, with particular reference to the Cretaceous evolution of the Japanese Islands, *in* Treloar, P.J., and O'Brien, P.J., eds., What drives metamorphism and metamorphic relations?: Geological Society [London] Special Publication 138, p. 137–169.

Caprarelli, G., and Leitch, E.C., 2002, MORB-like rocks in a Palaeozoic convergent margin setting, Northeast New South Wales, *in* Korsch, R.J., ed., 15th Australian geological convention symposium on the evolution of the Tasmanides, from supercontinent break-up to Tasman Sea opening: Australian Journal of Earth Sciences, v. 49, p. 367–374.

Catlos, E.J., and Sorensen, S.S., 2003, Phengite-based chronology of K- and Ba-rich fluid flow in two paleosubduction zones: Science, v. 299, p. 92–95.

Church, S.E., and Tatsumoto, M., 1975, Lead isotope relations in oceanic ridge basalts from the Juan de Fuca–Gorda Ridge area, N.E. Pacific Ocean: Contributions to Mineralogy and Petrology, v. 53, p. 253–279.

Cloos, M., 1985, Thermal evolution of convergent plate-margins: Thermal modeling and re-evaluation of isotopic Ar-ages for blueschists in the Franciscan Complex of California: Tectonics, v. 4, p. 421–433.

Coleman, R.G., and Lanphere, M.A., 1971, Distribution and age of high-grade blueschists, associated eclogites, and amphibolites from Oregon and California: Geological Society of America Bulletin, v. 82, p. 2397–2412.

Crawford, A.J., Falloon, T.J., and Green, D.H., 1989, Classification, petrogenesis and tectonic setting of boninites, *in* Crawford, A.J., ed., Boninites and related rocks: Boston, Unwin Hyman, p. 1–49.

DeBari, S.M., Taylor, B., Spencer, K., and Fujioka, K., 1999, A trapped Philippine Sea Plate origin for MORB from the inner slope of the Izu-Bonin Trench: Earth and Planetary Science Letters, v. 174, p. 183–197.

Dickinson, W.R., 1970, Relations of andesites, granites and derivative sandstones to arc-trench tectonics: Reviews of Geophysics and Space Physics, v. 8, p. 813–860.

Dickinson, W.R., Schweickert, R.A., and Ingersoll, R.D., 1996, Coast Range ophiolite as backarc/interarc basin lithosphere: GSA Today, v. 6, no. 2, p. 2–3.

Elderfield, H., and Pagett, R., 1986, Rare earth elements in ichthyoliths: Variations with redox conditions and depositional environments: Science of the Total Environment, v. 49, p. 175–197.

Erickson, R.C., Mattinson, J., Dumitru, T.A., and Sharp, W.D., 2004, Petrology, isotope geochemistry, and geochronology of a multiply-metamorphosed granitoid exotic block in a Franciscan olistostrome melange, Cazadero, California: Geological Society of America Abstracts with Programs, v. 36, no. 4, p. 39.

Ernst, W.G., 1970, Tectonic contact between the Franciscan melange and the Great Valley Sequence, crustal expression of a Late Mesozoic Benioff Zone: Journal of Geophysical Research, v. 75, p. 886–902.

Ernst, W.G., 1971a, Do mineral parageneses reflect unusually high-pressure conditions of Franciscan metamorphism?: American Journal of Science, v. 270, p. 81–108.

Ernst, W.G., 1971b, Metamorphic zonations on presumably subducted lithospheric plates from Japan, California, and the Alps: Contributions to Mineralogy and Petrology, v. 34, p. 43–59.

Ernst, W.G., 1984, Californian blueschists, subduction, and the significance of tectonostratigraphic terranes: Geology, v. 12, p. 436–440.

Ernst, W.G., 1988, Tectonic history of subduction zones inferred from retrograde blueschist *P-T* paths: Geology, v. 16, p. 1081–1084.

GEOROC database, http://georoc.mpch-mainz.gwdg.de/Entry.html.

Giaramita, M.J., and Sorensen, S.S., 1994, Primary fluids in low-temperature eclogites; evidence from two subduction complexes (Dominican Republic, and California, USA): Contributions to Mineralogy and Petrology, v. 117, p. 279–292.

Giaramita, M., MacPherson, G.J., and Phipps, S.P., 1998, Petrologically diverse basalts from a fossil oceanic forearc in California: The Llanada and Black Mountain remnants of the Coast Range ophiolite: Geological Society of America Bulletin, v. 110, p. 553–571.

Godfrey, N.J., and Dilek, Y., 2000, Mesozoic assimilation of oceanic crust and island arc into the North American continental margin in California and Nevada: Insights from geophysical data, *in* Dilek, Y., et al., eds., Ophiolites and oceanic crust: New insights from field studies and ocean drilling: Geological Society of America Special Paper 349, p. 365–382.

Godfrey, N.J., and Klemperer, S.L., 1998, Ophiolitic basement to a forearc basin and implications for continental growth: The Coast Range/Great Valley ophiolite: Tectonics, v. 17, p. 558–570.

Hacker, B.R., 1991, The role of deformation in the formation of metamorphic gradients; ridge subduction beneath the Oman Ophiolite: Tectonics, v. 10, p. 455–473.

Hamilton, W.B., 1969, Mesozoic California and underflow of the Pacific mantle: Geological Society of America Bulletin, v. 80, p. 2409–2430.

Hanan, B.B., and Schilling, J.-G., 1989, Easter microplate evolution: Pb isotope evidence: Journal of Geophysical Research, v. 94, p. 7432–7448.

Hanan, B.B., Kimbrough, D.L., Renne, P.R., and Shervais, J.W., 1991, The Stonyford Volcanic Complex: Pb isotopes and $^{40}Ar/^{39}Ar$ ages of volcanic glasses from a Jurassic seamount in the northern Coast Ranges: Geological Society of America Abstracts with Programs, v. 23, no. 5, p. 395.

Hanan, B.B., Kimbrough, D.L., and Renne, P.R., 1992, The Stonyford Volcanic Complex: A Jurassic seamount in the Northern California Coast Ranges: American Association of Petroleum Geologists Bulletin, v. 76, p. 421.

Hart, S.R., and Staudigel, H., 1989, Isotopic characterization and identification of recycled components, *in* Hart, S.R., and Gulen, L., eds., Crust mantle recycling at convergence zones: Dordrecht-Boston, D. Reidel, p. 15–28.

Hawkesworth, C.J., O'Nions, R.K., Pankhurst, R.J., Hamilton, P.J., and Evensen, N.M., 1977, A geochemical study of island-arc and back-arc tholeiites from the Scotia Sea: Earth and Planetary Science Letters, v. 36, p. 253–262.

Hofmann, A.W., Jochum, K.P., and White, W.M., 1986, Nb and Pb in oceanic basalts: New constraints on mantle evolution: Earth and Planetary Science Letters, v. 79, p. 33–45.

Hopson, C.A., Pessagno, E.A., Jr., Mattinson, J.M., Luyendyk, B.P., Beebe, W., Hull, D.M., Munoz, I.M., and Blome, C.D., 1996, Coast Range ophiolite as paleoequatorial mid-ocean lithosphere: GSA Today, v. 6, no. 2, p. 3–4.

Jakes, P., and Gill, J., 1970, Rare earth elements and the Island Arc Tholeiitic Series: Earth and Planetary Science Letters, v. 9, p. 17–28.

Johnson, L.E., and Fryer, P., 1990, The first evidence for MORB-like lavas from the outer Mariana forearc; geo-

chemistry, petrography and tectonic implications: Earth and Planetary Science Letters, v. 100, p. 304–316.
Krogh, E.J., Oh, C.W., and Liou, J.G., 1994, Polyphase and anticlockwise *P-T* evolution for Franciscan eclogites and blueschists from Jenner, California, USA: Journal of Metamorphic Geology, v. 12, p. 121–134.
MacPherson, G.J., 1983, The Snow Mountain complex: An on-land seamount in the Franciscan terrain, California: Journal of Geology, v. 91, p. 73–92.
MacPherson, G.J., Phipps, S.P., and Grossman, J.N., 1990, Diverse sources for igneous blocks in Franciscan melanges, California Coast Ranges: Journal of Geology, v. 98, p. 845–862.
Magaritz, M., and Taylor, H.P., Jr., 1976, Oxygen, hydrogen and carbon isotope studies of the Franciscan formation, Coast Ranges, California: Geochimica et Cosmochimica Acta, v. 40, p. 215–234.
Manning, C.E., and Bohlen, S.R., 1991, The reaction titanite + kyanite = anorthite + rutile and titanite-rutile barometry in eclogites: Contributions to Mineralogy and Petrology, v. 109, p. 1–9.
Maruyama, S., and Liou, J.G., 1988, Petrology of Franciscan metabasites along the jadeite-glaucophane type facies series, Cazadero, California: Journal of Petrology, v. 29, p. 1–37.
Maruyama, S., Liou, J.G., and Sasakura, Y., 1985, Low-temperature recrystallization of Franciscan greywackes from Pacheco Pass, California: Mineralogical Magazine, v. 49, p. 345–355.
Mattinson, J.M., and Hopson, C.A., 1992, U-Pb ages of the Coast Range ophiolite: A critical reevaluation based on new high-precision Pb-Pb ages: American Association of Petroleum Geologists Bulletin, v. 76, p. 425.
Meijer, A., 1976, Pb and Sr isotopic data bearing on the origin of volcanic rocks from the Mariana island-arc system: Geological Society of America Bulletin, v. 87, p. 1358–1369.
Miller, D.M., Goldstein, S.L., and Langmuir, C.H., 1994, Cerium/lead and lead isotope ratios in arc magmas and the enrichment of lead in the continents: Nature, v. 368, p. 514–520.
Moore, D.E., 1984, Metamorphic history of a high-grade blueschist exotic block from the Franciscan Complex, California: Journal of Petrology, v. 25, p. 126–150.
Moore, D.E., and Blake, M.C., Jr., 1989, New evidence for polyphase metamorphism of glaucophane schist and eclogite exotic blocks in the Franciscan Complex, California and Oregon: Journal of Metamorphic Geology, v. 7, p. 211–228.
Moores, E., 1970, Ultramafics and orogeny, with models of the US Cordillera and the Tethys: Nature, v. 228, p. 837–842.
Mueller, S., and Phillips, R.J., 1991, On the initiation of subduction: Journal of Geophysical Research, v. 96, p. 651–665.
Nelson, B.K., 1991, Sediment-derived fluids in subduction zones; isotopic evidence from veins in blueschist and eclogite of the Franciscan Complex, California: Geology, v. 19, p. 1033–1036.
Nelson, B.K., 1995, Fluid flow in subduction zones; evidence from Nd- and Sr-isotope variations in metabasalts of the Franciscan Complex, California: Contributions to Mineralogy and Petrology, v. 119, p. 247–262.
Page, F.Z., Mukasa, S.B., Essene, E.J., and Carrigan, C.W., 2003, Lu-Hf and U-Pb chronology of a possible Triassic Franciscan high-grade block, Healdsburg, California: Eos (Transactions, American Geophysical Union), v. 84, p. F1567.
Peacock, S.M., 1990, Fluid processes in subduction zones: Science, v. 248, p. 329–337.
Pearce, J.A., Thirlwall, M.F., Ingram, G., Murton, B.J., Arculus, R.J., and van der Laan, S.R., 1992, Isotopic evidence for the origin of boninites and related rocks drilled in the Izu-Bonin (Ogasawara) forearc, Leg 125: Proceedings of the Ocean Drilling Program, Bonin Mariana region; covering Leg 125 of the cruises of the Drilling Vessel *JOIDES Resolution,* Apra Harbor, Guam, to Tokyo, Japan, sites 778–786, 15 February 1989–17 April 1989, v. 125, p. 237–261.
PETDB database, http://petdb.ldeo.columbia.edu/petdb/.
Platt, J.P., 1975, Metamorphic and deformational processes in the Franciscan Complex, California: Some insights from the Catalina Schist terrane: Geological Society of America Bulletin, v. 86, p. 1337–1347.
Ridley, W.I., Perfit, M.R., Jonasson, I.R., and Smith, M.F., 1994, Hydrothermal alteration in oceanic ridge volcanics; a detailed study at the Galapagos fossil hydrothermal field: Geochimica et Cosmochimica Acta, v. 58, p. 2477–2494.
Ross, J.A., and Sharp, W.D., 1986, $^{40}Ar/^{39}Ar$ and Sm/Nd dating of garnet amphibolite in the Coast Ranges, California: Eos (Transactions, American Geophysical Union), v. 67, p. 1249.
Ross, J.A., and Sharp, W.D., 1988, The effects of sub-blocking temperature metamorphism on the K/Ar systematics of hornblendes: $^{40}Ar/^{39}Ar$ dating of polymetamorphic garnet amphibolite from the Franciscan Complex, California: Contributions to Mineralogy and Petrology, v. 100, p. 213–221.
Ryerson, F.J., and Watson, E.B., 1987, Rutile saturation in magmas: Implication for Ti-Nb-Ta depletion in island arc basalts: Earth and Planetary Science Letters, v. 86, p. 225–239.
Saleeby, J.B., 1992, Petrotectonic and paleogeographic settings of U.S. Cordilleran ophiolites, *in* Burchfiel, B.C., et al., eds., The Cordilleran Orogen; conterminous U.S.: The Geology of North America, Decade of North American Geology, Geological Society of America, v. G-3, p. 632–682.
Schweickert, R.A., and Cowan, D.S., 1975, Early Mesozoic tectonic evolution of the western Sierra Nevada, California: Geological Society of America Bulletin, v. 86, p. 1329–1336.
Sharma, M., Basu, A.R., and Nesterenko, G.V., 1992, Temporal Sr-, Nd-, and Pb-isotopic variations in the Siberian flood basalts; implications for the plume-source characteristics: Earth and Planetary Science Letters, v. 113, p. 365–381.
Sharp, W.D., and Leighton, C.W., 1987, Accretion of the Foothills ophiolite, western Sierra Nevada foothills, California: Geological Society of America Abstracts with Programs, v. 19, no. 6, p. 450.
Shervais, J.W., 1990, Island arc and ocean crust ophiolites; contrasts in the petrology, geochemistry and tectonic style of ophiolite assemblages in the California Coast Ranges, *in* Malpas, J., et al., eds., Ophiolites, oceanic crustal analogues: Proceedings of the Symposium "Troodos 1987": Nicosia, Cyprus, Geological Survey Department, Ministry of Agriculture and Natural Resources, p. 507–520.
Shervais, J.W., 2001, Birth, death, and resurrection: The life cycle of supra subduction zone ophiolites: Geochemistry, Geophysics, Geosystems, v. 2, p. 2001.
Shervais, J.W., and Kimbrough, D.L., 1985, Geochemical evidence for the tectonic setting of the Coast Range ophiolite: A composite island arc–oceanic crust terrane in western California: Geology, v. 13, p. 35–38.
Shervais, J.W., and Kimbrough, D.L., 1987, Alkaline and transitional subalkaline metabasalts in the Franciscan Complex melange, California, *in* Morris, E.M., and Pasteris, J.D., eds., South-Central Section meeting on alkalic rocks and kimberlites: Geological Society of America Special Paper 215, p. 165–182.
Shervais, J.W., Murchey, B.L., Kimbrough, D.L., Renne, P.R., and Hanan, B., 2005, Radioisotopic and biostratigraphic age relations in the Coast Range Ophiolite, northern California: Implications for the tectonic evolution of the Western Cordillera: Geological Society of America Bulletin, v. 117, p. 633–653.
Shimizu, H., Kunimaru, T., Yoneda, S., and Adachi, M., 2001, Source and depositional environments of some Permian and Triassic cherts; significance of Rb-Sr and Sm-Nd isotopic and REE abundance data: Journal of Geology, v. 109, p. 105–125.
Sisson, V.B., and Pavlis, T.L., 1993, Geologic consequences of plate reorganization; an example from the Eocene Southern Alaska fore arc: Geology, v. 21, p. 913–916.
Sorensen, S.S., Grossman, J.N., and Perfit, M.R., 1997, Phengite-hosted LILE enrichment in eclogite and related rocks; implications for fluid-mediated mass transfer in subduction zones and arc magma genesis: Journal of Petrology, v. 38, p. 3–34.
Stern, R.J., and Bloomer, S.H., 1992, Subduction zone-infancy: Examples from the Eocene Izu-Bonin-Mariana and Jurassic California arcs: Geological Society of America Bulletin, v. 104, p. 1621–1636.
Swanson, N., Erickson, R.C., and Plummer, E., 2004, Trace element geochemistry of the Ward Creek Metamorphic Sequence and Big Oat Creek Metabasalt, Cazadero, CA: Geological Society of America Abstracts with Programs, v. 36, no. 4, p. 39.
Tatsumi, Y., and Eggins, S., 1995, Subduction zone magmatism: Oxford, Blackwell Science, 211 p.
Tatsumoto, M., 1978, Isotopic composition of lead in oceanic basalts and its implications to mantle evolution: Earth and Planetary Science Letters, v. 38, p. 63–87.
Taylor, H.P., and Coleman, R.G., 1968, O^{18}/O^{16} ratios of coexisting minerals in glaucophane-bearing metamorphic rocks: Geological Society of America Bulletin, v. 79, p. 1727–1756.
Tribuzio, R., Messiga, B., Vannucci, R., and Bottazzi, P., 1996, Rare earth element redistribution during high-pressure–low-temperature metamorphism in ophiolitic Fe-gabbros (Liguria, northwestern Italy): Implications for light REE mobility in subduction zones: Geology, v. 24, p. 711–714.
Wakabayashi, J., 1990, Counterclockwise *P-T*-t paths from amphibolites, Franciscan Complex, California: Relics from the early stages of subduction zone metamorphism: Journal of Geology, v. 98, p. 657–680.
Wakabayashi, J., 1992, Nappes, tectonics of oblique plate convergence, and metamorphic evolution related to 140 million years of continuous subduction, Franciscan Complex, California: Journal of Geology, v. 100, p. 19–40.
Wakabayashi, J., 1999, Subduction and the rock record: Concepts developed in the Franciscan Complex, California, *in* Sloan, D., et al., eds., Classic Cordilleran concepts: A view from California: Geological Society of America Special Paper 338, p. 123–133.
Wakabayashi, J., and Deino, A., 1989, Laser-probe $^{40}Ar/^{39}Ar$ ages from high grade blocks and coherent blueschists, Franciscan Complex, California: Preliminary results and implications for Franciscan tectonics: Geological Society of America Abstracts with Programs, v. 21, no. 4, p. A267.
Wakabayashi, J., and Dilek, Y., 2000, Spatial and temporal relations between ophiolites and their subophiolitic soles: A test of models of forearc ophiolite genesis, *in* Dilek, Y., et al., eds., Ophiolites and oceanic crust: New insights from field studies and ocean drilling: Geological Society of America Special Paper 349, p. 53–64.
Wakabayashi, J., and Dilek, Y., 2003, What constitutes "emplacement" of an ophiolite?: Mechanisms and relationship to subduction initiation and formation of metamorphic soles, *in* Dilek, Y., and Robinson, P.T., eds., Ophiolites in Earth history: Geological Society [London] Special Publication 218, p. 427–447.
White, W.M., Hofmann, A.W., and Puchelt, H., 1987, Isotope geochemistry of Pacific mid-ocean ridge basalt: Journal of Geophysical Research, v. 92, p. 4881–4893.

Manuscript Received by the Society 18 February 2004
Revised Manuscript Received 9 December 2004
Manuscript Accepted 6 January 2005

Printed in the USA